YUNIBESITI YA BOKONE-BOPHIRIMA
NORTH-WEST UNIVERSITY
NOORDWES-UNIVERSITEIT

A Preliminary Theoretical Flutter Analysis of the JS1 glider

JA de Bruyn, B.Eng (Mech)

Thesis submitted in the School for Mechanical and Material Engineering at the North West University in partial fulfilment of the requirements for the Master's degree in Engineering.

Study Leader: **Mr AS Jonker**

Potchefstroom
November 2004

Abstract

A preliminary theoretic flutter analysis of the new JS1 18m-class glider was performed by means of analytic methods. This analysis consisted of a detailed modal analysis using finite element modelling followed by the flutter prediction.

The modal analysis was computed with the aid of the commercial FE-code ANSYS in which a model of the complete glider was generated. This model was created in such a way as to effectively simulate the composite characteristics, while also ensuring that the results were easily extractable for flutter prediction input. By using the Block-Lanczos method, the 1st, 2nd and 3rd main wing bending and torsion modes as well as the T-tail configuration modes were all extracted in the frequency range from 0 – 30 Hz. These modal results, which included the natural frequencies, mode shapes and displacements were then used as the input for the flutter code.

The flutter prediction was done with the software code SAF (Subsonic Aerodynamic Flutter). This prediction made use of a complete panel model for the glider, while the flutter algorithm was solved with the p-k method. The flutter results, in the form of V-g and V-f graphs, all showed main mode stability over the entire velocity range of $1.2V_D$ up to an altitude of 25000 ft.

Uittreksel

'n Voorlopige teoretiese studie van die "fladder"-eienskappe (Vloei-struktuur interaksie) van die pas ontwerpte JS1-sweeftuig is met behulp van teoretiese metodes uitgevoer. Die studie het bestaan uit 'n gedetailleerde modale analise, wat van die eindige element metode gebruik gemaak het, gevolg deur die fletter berekening.

Die modale analise van die volledige sweeftuig is bereken met behulp van die kommersiële eindige elementpakket, ANSYS. Die volledige model is op só 'n wyse opgestel dat dit die eienskappe van die saamgestelde materiaal realisties simuleer. Die model is verder ook geskep met inagneming van die modale inligting wat later verwerk moet word. Die analise is uitgevoer met die Block-Lanczos oplos-metode wat die eerste, tweede en derde hoofvlerkfrekwensies sowel as die T-stert konfigurasiemodusse binne die reeks 0 – 30Hz gevind het. Hierdie resultate, wat die natuurlike frekwensies, modusvorms en verplasings insluit, is toe gebruik as inset vir die fletter ondersoek.

Die fletter ondersoek het van die SAF-kode (*Subsonic Aerodynamic Flutter*) en 'n volledige paneelmodel van die sweeftuig gebruik gemaak, terwyl die algoritme met die p-K metode opgelos is. Die resultate van die studie, in die vorm van V-g en V-Hz grafieke, het almal stabiliteit getoon tot 1.2 keer die ontwerpspoed V_D en tot 'n hoogte van 25000 vt bo seespieël.

Acknowledgements

I would like to thank God who has provided me with the ability to perform this study as well as my promoter, Attie Jonker and every one else who gladly shared their knowledge with me.

Table of Contents

List of Figures

List of Tables

Introduction

1.1. Preface

The history of flight can be traced back more than 100 years. It all started with pioneers such as Otto Lilienthal and the Wright Brothers. These designers were fascinated by the idea of flight, but, though they achieved it, had little or no understanding of the interaction between elastic structures and aerodynamic forces. As the aviation industry got off the ground they soon began to experience a new phenomenon where the self-excitation of certain lifting surfaces occurred at different flight speeds. This occurrence was called flutter and saw a dramatic increase as better engines became available from the 1930s. Consequently, serious engineering effort was put into analysing and preventing flutter, especially with regard to the faster and more complex aircrafts of the years to follow. Early attempts at reducing flutter were mainly aimed at increasing the stiffness of the structure and control surfaces, and included extensive wire bracing (Hollmann, 1997:3). These external methods provided moderate success with biplanes, but with the shift to cantilevered wings after World War I, it became apparent that it would be necessary to find analytic flutter prediction methods.

Before the development of analytic methods, there were no real formal flutter testing procedures for full scale aircraft. Testing was done by simply flying the plane to its maximum stability speed (Kehoe, 1995:1). This hazardous situation was mainly due to inadequate instrumentation, excitation methods and stability determination techniques. Traditional techniques were inefficient as well as unsystematic and were not always able to predict flutter occurrence.

However, analyis has come a long way over the years, and today's aircraft designs undergo sophisticated aeroelastic analyses to ensure that designs are flutter-free within the design flight envelope. These analyses were made possible by analytic algorithms incorporated into software codes such as SAF, ZAero and others, as well as advanced measuring and data extraction techniques.

Performing a flutter analysis of a newly designed aircraft is still no easy task, but with the availability of the above tools it is within the reach of relatively inexperienced designers. This project will utilise the resources mentioned, as well as alternative methods of data analysis, in order to provide a preliminary flutter analysis of the newly designed 18m-class all composite glider.

1.2. Problem Definition

The North-West University (South Africa) is currently developing a new 18m-class glider (see Appendix A4). This glider makes use of a fuselage similar to the ASH26. In order to certify the new aircraft, an analytical flutter test needs to be performed.

The flutter analysis comprises obtaining the natural frequencies and the associated displacements of the aircraft structure under investigation. The results are then used in conjunction with an aerodynamic model in a flutter code to predict the flight speeds at which self-excitation will start for the different modes. The lowest speed at which excitation starts is denoted as the critical speed or flutter-speed of the aircraft.

1.3. Objectives of this study

The overall objective of this study is to provide the development team with a first theoretic flutter report in terms of the JS1 glider under development. This first analysis will include only the main lifting surfaces with the possibility of adding control surface at a later stage.

Normally the flutter investigation would be performed after the completion of the aircraft, but for this project it was decided to perform it concurrent with the prototype development. This will aid the developers and allow them to make changes to the aircraft structure before building the actual prototype, thus saving on development costs and time.

The complete analysis will be divided into two main sections, namely the modal analysis and the flutter prediction procedure.

1.3.1. Modal Analysis

Every structure that consists of both mass and stiffness properties has a unique set of vibration characteristics. This includes the natural frequencies as well as the associated mode shape displacements of the structure. These characteristics are further influenced by the damping of the structure which is mostly taken as a fixed value. The process of determining these quantities is called a modal analysis, and it can be performed by means of either a ground vibration test or analytic methods.

Ground vibration tests are performed on complete aircraft structures by exciting the lifting surfaces while measuring the wing displacements with accelerometers. Alternatively, the quantities can also be determined by means of an analytic procedure as incorporated into the finite element method. This study will make use of a complete finite element model to determine the modal characteristics, for the reasons set out described in the previous section.

The mode shape displacements, together with the natural frequencies of the different modes, are then used as the input into the flutter prediction code which determines any instability. Figure 1 shows where exactly a modal analysis fits into the picture.

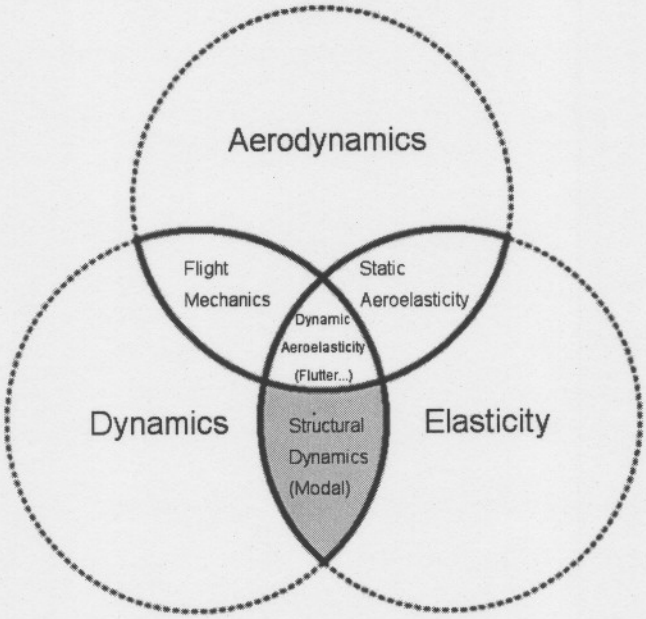

Figure 1: Schematic of the field of aeroelasticity (Hodges, 2002)

The next section will provide an overview of the coupling of the modal results with the aerodynamically induced forces.

1.3.2. Flutter prediction

The flutter prediction section of this project will involve using the modal analysis data together with an aerodynamic model in a flutter analysis code. This code will be used to solve the coupled analysis and predict the airspeed at which the first signs of flutter appear, as well as any susceptible modes.

The flutter code that will be used is SAF (***S**ubsonic **A**erodynamic **F**lutter*), which is a modification of the original flutter code FASTOP (***F**lutter **A**nd **St**rength **O**ptimization **P**rogram*). This original code was developed by Grumman Aerospace Corporation, New York, under the supervision of the Air Force Flight Dynamics Laboratory at Wright Patterson Air Force Base in Ohio, and later modified by Aircraft Design Inc. to run on a personal computer.

1.4. Limitations of the study

Due to the fact that this thesis is submitted in partial fulfillment only of a Master's degree in Engineering, it will be limited to the following:

- The preliminary flutter analysis will only be performed for the main lifting surfaces, thus excluding control surface flutter investigations.

1.5. Layout of the thesis

In Chapter 2: Literature Study, the design specifications, modal analysis options and flutter prediction methods will be discussed. Chapter 3: Modal analysis will be devoted to the methods implemented to achieve a modal analysis of the complete sailplane. Chapter 4: Flutter Prediction will utilise the chosen flutter tool to predict the flutter and verify that it complies with aviation requirements, while Chapter 5: Conclusion will provide a short overview of the thesis with suggestions for further research.

2 Literature Study

2.1. Introduction

Aeroelasticity can be described as a study concerning the interaction between the inertia, elasticity and aerodynamics of a specific structure. It is within this interaction that structures start oscillating at large amplitudes and stresses, due to energy being exchanged between the different modes of the structure. This instability is called flutter, and can be responsible for causing anything from minor discomfort to instant structural failures.

It has been accepted for years that high speed aircraft are more susceptible to flutter, but history has taught us that no speed regime is quite immune. References (Collar, 1978; Tolve, 1958; and Garrick, 1981) give many examples of accidents. With the introduction of thinner wings and T-tail configurations the likelihood of flutter within the envelope increased drastically, which emphasises the need for finding alternatives to the traditional prediction methods. Traditional methods focused more on testing completed aircrafts using different in-flight techniques. In answer to this problem, a series of analytic methods were developed, and these are still employed today, along with some traditional methods. The combination ensures a more detailed level of pre-flight investigation, which again increases the safety of the actual flight test.

This chapter will give an overview of these methods as well as a clear indication of which methods will be employed during this specific preliminary flutter analysis. The analysis specification, as provided by Aviation Authorities, will also be discussed and will serve as the guideline throughout the rest of this study.

2.2. Analysis Specifications

The first step in the flutter analysis process in respect of a new aircraft is to know which requirements need to be satisfied. The Joint Aviation Requirements (JAR) study-group

is an organisation that sets standards for the design, manufacturing and testing of all aircraft as well as sailplanes. JAR-22 will be used for the specifications of this study.

The following section will be devoted to a discussion of said requirements as well as how these are to be implemented in this study.

2.2.1. Joint Aviation Requirements (JAR)

The JAR-22 states that a new glider has to comply with the flutter standards as described in section 22.629 before application for certification can begin:

- The sailplane must be free from flutter, airfoil divergence and control reversal in each configuration and at each appropriate speed up to at least V_D (Design velocity). Sufficient damping must be available at any appropriate speed so that aeroelastic vibration dies away rapidly (JAA, 2003:63).

Compliance to this standard can be shown by a ground vibration test (GVT) as well as an analytical method. It should be possible, with the analytical method, to predict the critical flutter speed in the range up to 1.2 times the design speed and then to follow up with an actual flight test. This flight test must be performed in order to induce flutter at speeds up to V_D, from which it must be shown that the damping margin is suitable. A detailed description of a flutter flight test procedure is given by Kimberlin (2003).

The design velocity (V_D) of the JS1 sailplane under consideration in this study is 324km/h. In order to apply for certification, the applicant must therefore show that the sailplane is free from flutter up to 388.8 km/h. However, to perform this analysis, one first needs the results from a modal analysis. These two main groups – modal analysis and the actual flutter prediction – will form the basis for the layout of the rest of this chapter.

2.3. *Modal analysis*

The modal analysis is the first of two very important elements in the completion of this project. The main purpose of a modal analysis is to provide the natural frequencies of an elastic structure. A secondary purpose is to provide the modal displacement data associated with each mode, which can be extracted. Special care must be taken with regard to the accuracy of the extracted data, as the flutter prediction relies directly on it.

The process of performing a modal analysis can generally be divided into two different sections. The first refers to the more conventional methods that consist of performing actual experiments on completed aircrafts. These methods all include the three distinctive parts of structural excitation, response measurement and data analysis, all of which will be discussed next.

The second method is a more analytical method and relies more on computer simulation to calculate the structural response of the aircraft. Both these methods together with a section on flutter flight testing will now be discussed in this section, after which the Conclusion will provide a diagram of the proposed procedure that will be used during the scope of this project.

2.3.1. Conventional methods

The conventional ways of performing a modal analysis have seen some developments over the past 60 years, but still consist of the three basic parts first introduced by Von Schlippe (1936) – structural excitation, response measurement and data analysis. Each of these parts will now be discussed and evaluated with regard to this project.

2.3.1.1. Structural Excitation

Structural excitation refers to the application of a force to a given structure in order to excite all of the desired vibration modes. These modes need to be excited with sufficient magnitude to accurately assess the response data. An important aspect revealed by

history was the fact that excitation methods must provide not only adequate force levels but also adequate excitation over the desired range of frequencies, as well as being light weight, so as not to affect the modal characteristics (Kehoe, 1995:5).

This structural excitation process is performed either as part of a ground vibration test or as part of the actual flutter testing procedure. The following examples of excitation will refer only to methods used for GVT, as the output from these tests is the desired modal results. Structural excitation for the purpose of flutter prediction will be mentioned in 2.4.4.1

The first method is by means of an impact hammer. For this method the structure needs to be covered by multiple sensors where after it is hit by a modal impact hammer. This approach is used widely but might not provide all the desired natural frequencies. Using a steel tip will excite higher frequencies, where as a softer materials is used to for the lower frequencies.

Another method is by means of inertia shakers. This refers to eccentric oscillating weights creating forces that are proportional to the exciter weight multiplied by the square of the rotating speed. This method provided larger frequency bands and is typically used in ground vibration test to determine vibration characteristics from 5 to 50Hz (Kehoe, 1995).

2.3.1.2. Response measurement

Response measurement refers to the complete system of instrumentation used to record the structural responses of the airplane under a certain excitation. This response data must be obtained from enough locations and be of high enough quality. Included in the instrumentation system is the measurement, telemetry, recording and displaying of the response data.

The most common transducers used to measure the excited response of the structure have been accelerometers and strain-gauges, with accelerometers being the more

dominant of the two over the past few years. Thanks to the development of piezoelectric material these accelerometers became as small as 0.25 by 0.15 inches and as light as 1 gram (Nordwall, 1993). The small accelerometers also have the advantage of having a linear frequency range of 1 to 10 000 Hz, and they can operate in a temperature range of -65 to 200°F.

From this measurement equipment, the response data is transferred to a processing unit where the final component of the flutter testing process will be completed.

2.3.1.3. Data analysis

The last component of the modal analysis methodology is the analysis of the response signal, which will in the end serve as the final stability indication. This component included tasks such as filtering the response data for noise and separating closely spaced modes and symmetric / anti-symmetric modes. Until the 1950s, this was done by means of adding and subtracting time histories by hand (Philbrick, 1958), but the introduction of digital computers and programming algorithms such as the Fast Fourier Transformation (FFT) made it possible to obtain frequency content of acquired signals in less than a second.

2.3.2. Analytic modelling

Analytic modelling of a modal analysis by means of the finite element method (FEM) is becoming the alternative, or rather a complement to the conventional methods described in the previous section.

A modal analysis is now performed by setting up a very detailed finite element model of the structure in order to find the natural frequencies as well as the associated mode shapes. The weight and stiffness of the inspected lifting surfaces are matched to those of the actual aircraft, which ensure the accuracy of the final data. These natural frequencies can further be checked by means of a ground vibration test (GVT). The

mode shapes as well as the displacement data from the finite element analysis (FEA) are then used as input into a flutter prediction code.

For the purpose of this study, it has been decided to use the finite element modelling approach. This method was selected because a complete sailplane was not ready for a GVT yet, and it was felt that concurrent engineering between the manufacturing and flutter modelling could greatly enhance the final product. The commercial software code ANSYS was selected for the simulation, due to its availability at the University as well as for its technical ability. ANSYS provides several element types for the modelling of composite materials (ANSYS Inc., 2000) as well as six different methods of calculating the modal response of a structure. This analysis made use of the block Lanczos method suggested for large symmetrical problems (ANSYS Inc., 2000).

The next issue was that of the element type and geometry to be used. A comparative modal study of a simple beam, using triangular and rectangular elements, has shown that the rectangular elements were up to 15% more accurate than the former (Maurice, 1998). From this result it could be concluded that the first choice of elements would always be rectangular, with triangular only being used where the geometry would require it. With the element shape being chosen it will also be necessary to build up confidence in the accuracy as well the solution procedures of the chosen elements. Much work has been done on these element evaluation processes and Robinson (1985) even proposed a set of six tests that could be conducted in order to build confidence in the specific element. Examples of modal analyses allow us to conclude that a validation test followed by a convergence test is sufficient for most applications (Shokrieh et al, 2001). For the purpose of this study it was decided to validate the model by means of two independent finite element models. This validation will also be used to do a convergence analysis on the finite element model.

The different element types offered by ANSYS were all created with specific applications in mind. Although there were about five element types for composite modelling, the final choice was between the SHELL91 and SHELL99 elements. Both these elements had 6 degrees of freedom at each node (UX, UY, UZ, ROTX, ROTY, ROTZ) and could model up to 250 layers. Figure 2 shows the element formation and

stress recovery time as a function of the number of layers (ANSYS Inc., 2000). While SHELL91 uses less time for elements of under three layers, SHELL99 uses less time for elements with three or more layers. SHELL99 was therefore selected as the element type to be used during the modal analysis.

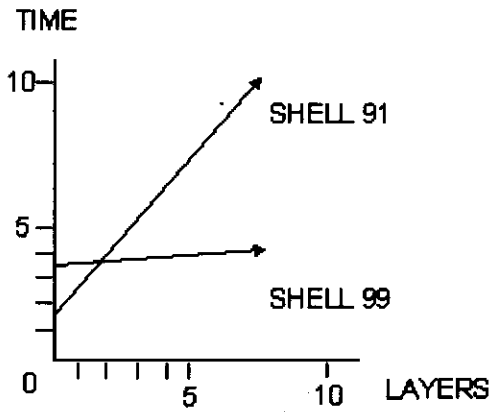

Figure 2: Comparison between SHELL99 & SHELL91 elements (ANSYS Inc., 2000)

2.4. Flutter Prediction

2.4.1. Introduction

The aircraft community spends considerable time and money to extend and increase the flight envelope of aircraft. For this reason, it has become an absolute necessity to be able to safely and accurately predict the speed associated with the onset of aeroelastic instabilities, or the more common phenomenon of flutter.

The following section will be devoted to several methods developed with the aim of predicting the onset of flutter while also mentioning some current flutter flight testing techniques. The development of these methods eliminated the need to rely completely on flight tests and included a variety of techniques which range from purely analytic to using only flight test data. Though all have been shown to be theoretically correct, a quick review will provide information regarding choosing the most appropriate one.

Before these prediction methods can be evaluated, one needs to understand something about the basics of the aeroelastic phenomenon called flutter. An introduction into aeroelasticity will be divided into static and dynamic aeroelasticity. Static aeroelasticity, although not evaluating the effect of inertia, will first be discussed, as this section provides the basic model to be used through this introduction. The next section will then give an overview of dynamic aeroelasticity, which is more specific to the phenomenon of flutter.

2.4.2. Static Aeroelasticity

Static aeroelasticity has to do with analysing the parameters affecting the interaction between a moving fluid and an elastic structure. The difference between static and dynamic is the exclusion of the inertia effect in the static determination (Hodges et al, 2002).

The system that will be used to introduce these parameters is the so-called "typical section" (Dowell et al, 1995), which consists of a rigid, flat plate airfoil mounted on a torsional spring attached to a wind tunnel wall. Figure 3 illustrates the geometry of this typical section.

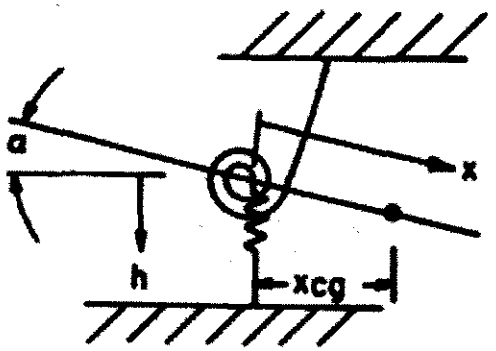

Figure 3: Typical Section (Dowell et al, 1995)

The main objective of this model for the aeroelastician is to determine the rotation of the plate as a function of the airspeed. A typical plot of these two parameters, the elastic twist vs. the airspeed, is given in figure 4, with U_D being the divergence speed (the speed where the elastic twist increases rapidly up to the point of failure). In this process one would like to predict U_D as accurately as possible.

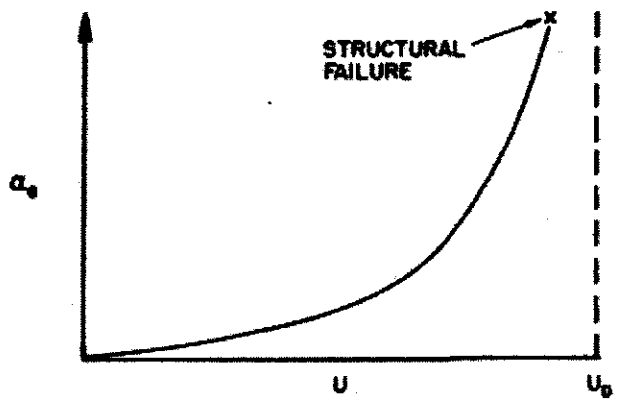

Figure 4: Typical twist vs. airspeed (Dowell et al, 1995)

This theoretical process of obtaining a prediction for U_D begins with the equation of static equilibrium which states that the sum of the aerodynamic plus elastic moments about any point of the airfoil is zero. This equation, the static equilibrium equation, is then solved for the elastic twist α_e, and has a few interesting properties. The most interesting property is perhaps the fact that the elastic twist becomes infinitely large at a particular dynamic pressure.

The dynamic pressure at which this occurs is known as the divergence dynamic pressure, and represents a corresponding air velocity at which the elastic twist can become so large as to cause structural failure. Because of this occurrence it is necessary to determine the divergence limits of all lifting surfaces and ensure that the aircraft always stays below those limits.

Static aeroelasticity is usually used for the prediction of the lift that is developed by an aircraft for a specific configuration or to determine the maximum load factor that the aircraft can sustain. For this reason, static aeroelasticity will only be treated as background to the dynamic side; which will be more appropriate to the flutter analysis.

2.4.3. Dynamic Aeroelasticity

Dynamic aeroelasticity on the other hand, recognises the importance of all the inertial forces, and takes them into account when deriving the governing equations. In order to discuss this phenomenon, it is necessary first to take a look at how this equation is obtained.

Using Newton's Second Law would seem like the obvious choice for obtaining the dynamic aeroelasticity equation, but it is not the preferred procedure. Instead, the alternatives mostly used today are those offered by Hamilton's Principle or Lagrange's Equations (scalar presentations of Newton's second law), the latter being used especially for its systematic and economic advantages with multi-freedom systems (Meirovitch, 1970). Equation 2.2 defines the Lagrange equations:

$$-\frac{d}{dt}\frac{\partial(T-U)}{\partial \dot{q}_i}+\frac{\partial(T-U)}{\partial q_i}+Q_i=0 \qquad i=1,\ 2,... \qquad (2.2)$$

With T being kinetic energy, U being potential energy and Q referring to the generalised aerodynamic forces.

To further increase the flexibility of this equation, the concept of "generalised" coordinates (q. in eq.2.2) was introduced. This refers to a coordinate that is arbitrary and independent of other coordinates. Turning again to the typical section (Fig. 3) the following two generalised coordinates are sufficient to describe the motion of the dynamical system:

Generalised coordinates:

$$q_1 = h$$
$$q_2 = \alpha$$

By assuming a sinusoidal motion for these two coordinates, the original Lagrange equation can be cast into an eigenvalue problem. Solving the eigenvalues (consisting of a real and an imaginary part) will eventually provide critical information about the stability of the dynamic system.

The following figures show the three typical characteristics of a dynamic system: (a) stable, (b) marginally stable and (c) unstable. For the aircraft to be stable, it must have the ability to dissipate the energy absorbed from the free stream, thus minimising the amplitude of the oscillation or damping the vibration. Where the aircraft exhibits marginal stability regarding oscillations, the amplitude of the oscillations will remain constant, and if the system is unstable, the oscillations will keep on increasing and eventual failure of the wing or airframe will occur.

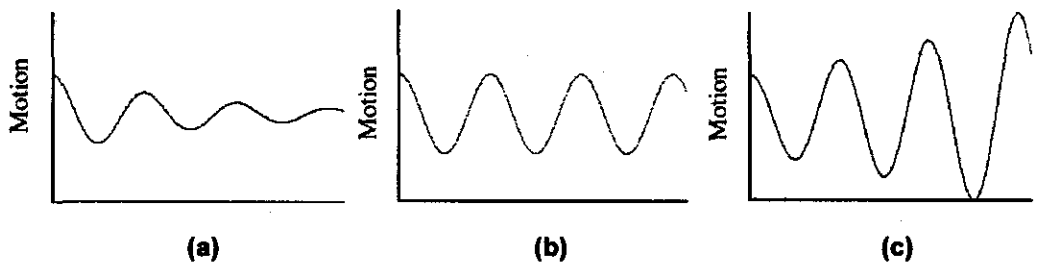

Figure 5: Stability (a), Marginal Stability (b), and Instability (c)

With this background in mind it is now necessary to look at some of the different methods used to predict flutter.

2.4.4. Flutter prediction methods

The following section will provide an evaluation of a few different flutter prediction methods. This will range from purely flight testing, with an introduction on varies structural excitation methods to purely analytical prediction. Among these methods will be algorithms based on damping extrapolation as well as solving the governing equations.

2.4.4.1. Flutter Flight Testing Techniques

Flight flutter testing was the only way to predict this onset of this phenomenon in the past and is still today the final task of a complete flutter analysis. These tests also consisted of the three distinct regions as mentioned in the 2.3. This section will however only refer to some of the structural excitation methods that are used while the sections to follow will provide more information on the actual prediction of flutter.

Over the years, many types of excitation systems have been used with varying degrees of success. Control surface pulses were probably the most common of the in-flight methods and were favoured because no special equipment was needed. This method can basically be described as a sudden movement of the control surfaces. Apart from the apparent advantages, the drawback to this method was the fact that the pilot would find it difficult to excite any modes above 10 Hz. In spite of its limitations, control surface pulses were continued up to the late 1950s, until it became evident that flight was possible beyond the flutter speed without exciting flutter with pulses (Stringham, 1958)

Another in-flight method that proved to have some degree of success was that of thrusters, or also known as bonkers. These small, single-shot solid-propellants had burn times of 18-24 ms and could generate thrust of up to 18 000 Newton. Thrusters had the advantage of being lightweight, but their single-shot capabilities and narrow frequency band were a disadvantage (Laure, 1974). The next sections will now provide a more in depth look at the actual methods of predicting the onset of flutter.

2.4.4.1.1. Damping Extrapolation

Modal damping extrapolation is probably the most commonly used method of predicting flutter (Lind, 2001), and can be regarded as a data-based procedure. This is due to the fact that the analysis relies completely on flight data, with no consideration of any theoretic models.

The method is quite simple to understand and is based on only the variation in the modal damping of the investigated surface. During flutter, the damping of at least one mode becomes zero, and by noting these variations, one can extrapolate to an airspeed at which flutter should occur. Figure 6 shows this procedure.

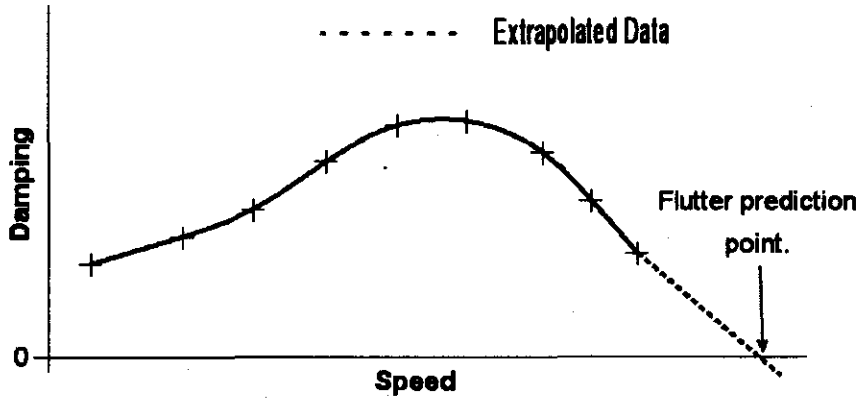

Figure 6: Damping Extrapolation Method

Although the principle is sound, there are some difficulties in implementing it. The first problem is that of damping extraction, which needs very sophisticated techniques in order to process the low signal-to-noise ratio. The other troublesome area is the extrapolation method. Damping is mostly a nonlinear function of airspeed which needs to be accounted for in the extrapolation scheme used.

2.4.4.1.2. Flutterometer

The flutterometer (Lind et al, 2000) is another tool to be discussed which differs to some extent from most other approaches. It uses a model-based approach which makes use of flight data as well as theoretic models to predict the onset of flutter. This approach, which is analytically predictive, provides a further enhancement over the questionable results from extrapolating nonlinear damping trends.

The flight data under consideration is frequency-domain transfer functions from sensors to an excitation, while the model formulation is based on the μ-method. A mathematic description of the μ-method is beyond the scope of this study and information may be found in the literature (Lind et al, 1999).

The initial step in the flutterometer procedure is to calculate an uncertainty parameter for the model at a specific test point. This is done by monitoring the differences between the measured and theoretic transfer functions and introducing them into the model. From here on the μ-method is simply implemented to compute the robust flutter speed. In this way, the flutterometer predicts a more realistic speed due to the implementation of flight data variations into the theoretic model.

Although this method does provide some superior results, it still has a few disadvantages. One of them is the fact that one will probably still need to do an analytic flutter analysis before conducting the flight test, in order to approach the flight test with the necessary care. Another is that modifications can only be made to the completed plane afterwards, compared to implementing changes during the manufacturing process.

2.4.4.2. Analytic Flutter Codes

Another method to be discussed is the implementation of a purely analytic code to evaluate the flutter characteristics of the investigated airplane. This method will be implemented during the scope of this study and will firstly be discussed with regards to the background of its calculations.

Over the years, flutter calculation methods have evolved from 3-D hand calculations assisted by tables of aerodynamic coefficients (Hollmann, 1997) to the implementation of modern algorithms in software codes. It was mostly the development of the mainframe computers that pushed aerospace companies to start creating software capable of predicting flutter much more accurately. Several of the more common methods implemented in today's software codes, as well the advantages and disadvantages of each of these, will now be presented.

The aerodynamic flow around an arbitrary body is analysed by dividing the geometry into individual panels, and is known as the panel method (Bosman, 2001). These panels each induce a velocity on itself as well as the remaining panels, and can be modelled by relatively simple equations. These equations are functions of geometric relationships such as distances and angles between the panels. Each panel's attributes are then written into a matrix and solved to satisfy the boundary conditions. This method provides an accurate alternative to Navier-Stokes solvers and has the advantage of being much less computer intensive.

On the solving side, only the following two methods will be discussed: K-method and the pK method. These methods represent the most common of all used today and will be discussed according to merits and technical validity. The basic equation of these methods is the dynamic aeroelastic equation described in section 2.4.3, which is now derived in the Laplace domain in terms of the generalised mass, stiffness and aerodynamic forces matrices.

The k-method (Hassig, 1971) was derived by replacing the Laplace parameter with an artificial complex structural damping parameter that is proportional to the stiffness. This addition was proposed by Theodorsen (1935) and was done in order to sustain the assumed harmonic motion. However, the formulation had a few drawbacks – such as the fact that the equation could not be solved for some trivial solutions associated with rigid body modes. Another drawback was the fact that the frequency and damping values sometimes "looped" around themselves, thus yielding multiple frequency and damping values as a function of the velocity. A further limitation was the fact that valid solutions could only be produced with no damping whatsoever.

The pK-method is the other well known procedure. This method represents the aerodynamic matrices as stiffness and damping matrices. The addition of this damping matrix is the main difference from the k-method. Advantages of the method are that it converges quite rapidly while also allowing the modelling of control systems. Damping values obtained in off-flutter conditions also appear to be more representative of the actual damping.

For the purpose of this study, it was decided to make use of the analytic model approach. This approach was selected because a complete glider was not yet ready for flight testing and because this procedure could greatly assist the first prototype. The commercial software code, SAF, was chosen for the flutter analysis, due to its implementation of the doublet lattice panel method as well as pK-solving algorithm. These were both properties recommended by an aeroelastician from the CSIR (Van Zyl, 2003). By using the verified FE-model, a realistic flutter prediction can now be made.

The following figure shows a flow chart of the overall aircraft certification procedure, with this preliminary flutter study indicated in gray. However, the final step of verifying the results with a complete GVT does not fall within the scope of this project.

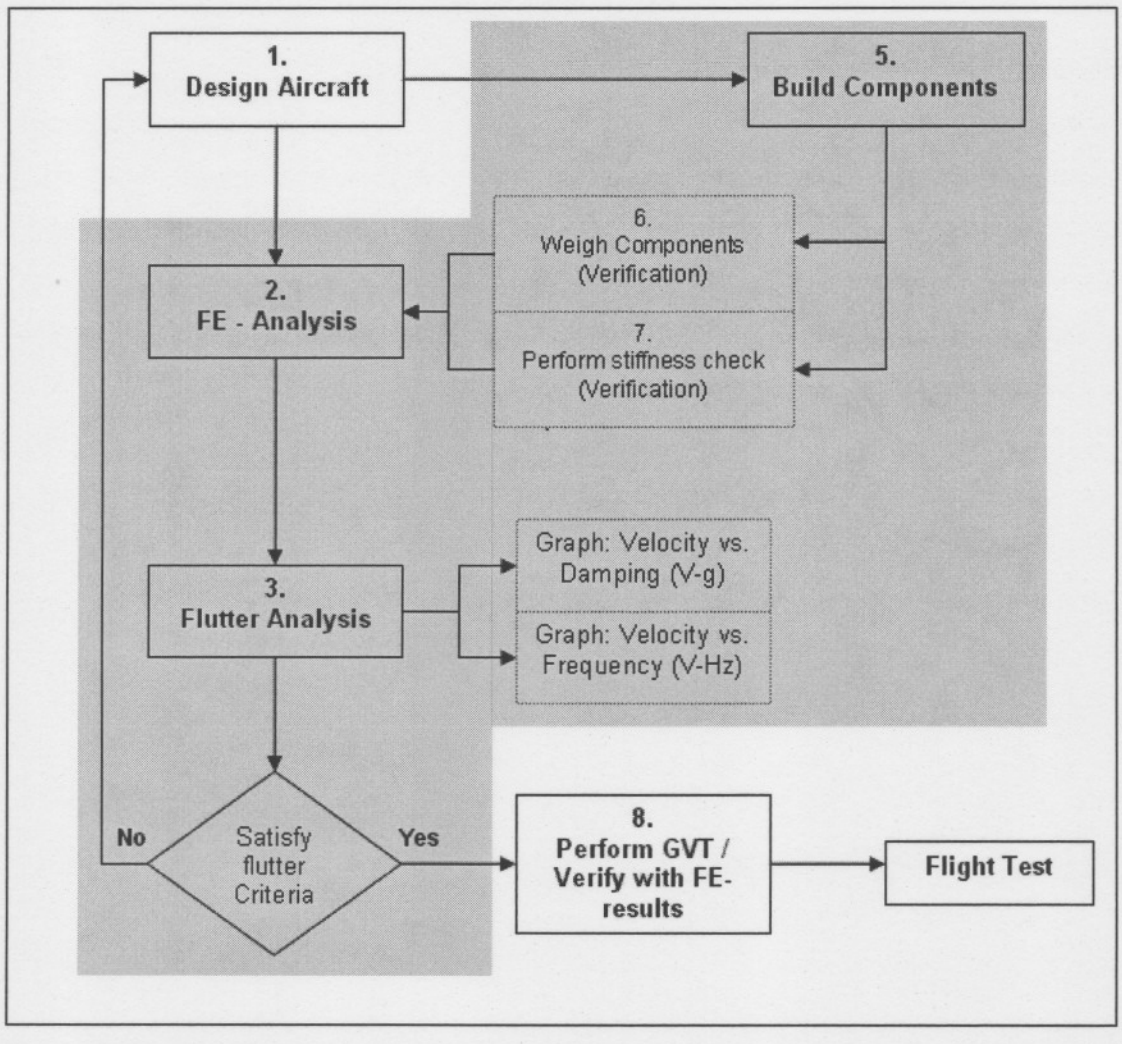

Figure 7: Flutter Analysis Flow Chart

2.5. *Summary*

This chapter provided the design specifications as well as some of the most applicable methods for performing a flutter analysis. These methods were discussed with regards to the modal analysis and the actual flutter prediction procedures. The advantages and disadvantages of such methods were given, and a brief overview of the fundamentals of flutter presented. The chapter ended with some design methodologies and also included the flowchart for this specific project.

3 Modal Analysis

3.1. Introduction

A modal analysis is performed to obtain the natural frequencies and associated mode shapes of an elastic structure. Traditionally this analysis was performed by ground vibration tests (GVTs) alone, while a more modern approach entails the incorporation of computer techniques prior to GVTs. These computer techniques refer to the application of the finite element modelling algorithm as well as the entire process that accompanies the creation of the analytic model.

This chapter will now provide an in-depth look into the process to be followed to create the modal analysis model which will provide the input with regard to the flutter code. The process can be broken down into three distinct sections, namely computer aided design modelling (CAD modelling), model verification and results generation. The chapter will also be presented in this order.

3.2. Modelling

3.2.1. Computer Aided Design Modelling (CAD modelling)

CAD modelling refers to the graphical designing or modelling of a structure in three-dimensional computer space. Such models can then be used in other software packages, such as Finite Element Codes, to perform various types of analysis.

In order to ensure that the properties, such as stiffness and weight, of the aircraft are realistically modelled, it is necessary to create a very accurate FE-model. This therefore means that the CAD-model needs to incorporate enough detail to make the model as realistic as possible. It was therefore decided to model the complete aircraft as a whole instead of modelling smaller components individually. The following points reflect some of the things that needed special attention during the CAD modelling process:

- Creating areas bounded by three or four straight lines.
- Preparing the CAD-model for different lay-up schedules.
- Preparing the CAD with data extraction points in mind.

Area Creation

The complete glider was modelled as a collection of surfaces in order to reduce the number of elements used. Surface modelling seemed more than adequate, since the length to thickness ratio of the areas was much larger than the recommended ratio of 4. All surfaces were created in such a way that they had either 3 or 4 straight line boundaries. This method proved to be the most efficient during importing stages and eased the meshing process considerably. Another important aspect of the area creation was the fact that neighboring areas had to share one common line with the same endpoints. Areas that did not meet this criterion caused a lot of problems regarding connectivity of adjacent regions and in the end needed to be replaced. Figure 8 a) shows three areas where Area 3 does not meet the criterion of sharing one common line and endpoints with its neighboring areas, while the correction is given in Figure 8 b).

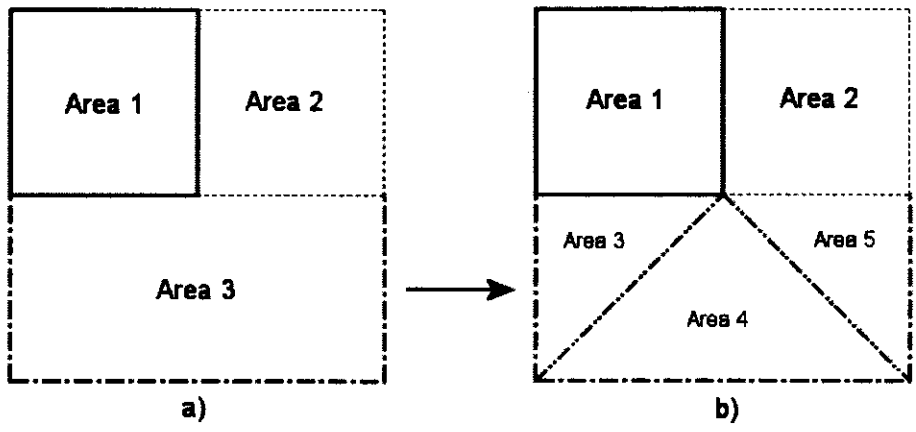

Figure 8: Optimal Area for FE-model

By implementing this procedure, the whole glider model was recreated and exported as an IGES file.

Different Lay-up Schedules

A lay-up schedule refers to the properties of composite material sections. Lay-up schedules consist of the material, orientation and angle of each layer in a specific section. The sailplane being a complete composite structure, it presented nearly 200 different sections, each with its own lay-up schedule. In order to accommodate these different lay-ups in the FE-model, the FE-software code makes use of predefined areas. This meant that apart from the guidelines set out in the previous paragraph, the CAD-model also needed to conform to the lay-up schedules as defined from a static analysis. Figure 9 shows a piece of the wing with the different colors representing areas where the lay-up changes.

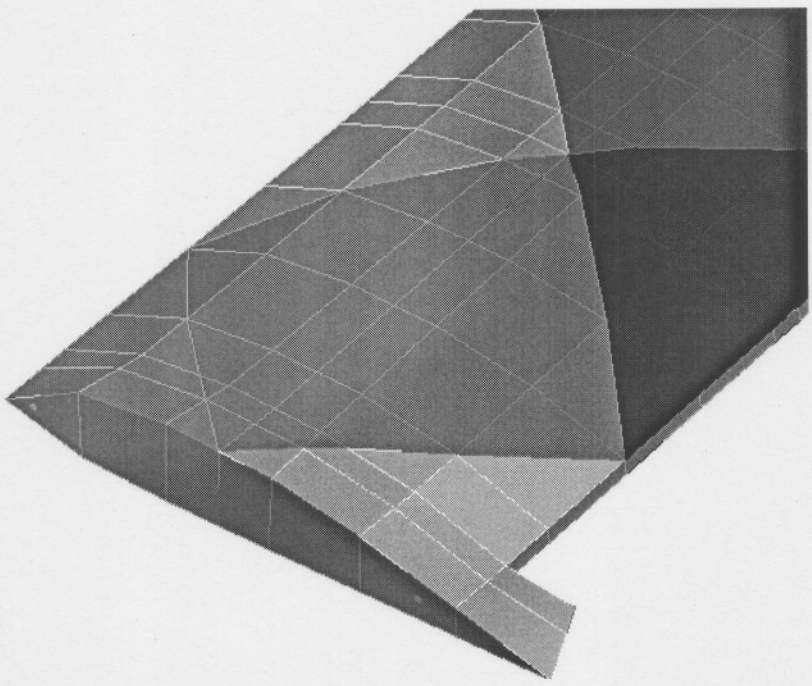

Figure 9: CAD Areas of Wing

The final point that needed to be considered during the CAD-modelling process was the modal data extraction points; this will be discussed next.

Modal Data Extraction Points

The flutter code, SAF (Subsonic Aviation Flutter) uses the z-displacements of a grid of points on the lifting surfaces. This grid is similar to the one created with accelerometers during a GVT, but again has a few restrictions. The modal data displacements must be entered along a spanwise line reaching from the fuselage centerline to the tip of the lifting surface, and a minimum of two lines are required. Since data was extracted from nodes, it was necessary to ensure the location of certain nodes. This was done by placing keypoints at the desired locations. A keypoint refers to the corner coordinate of an area and always has a node attached to it. Figure 10 shows a simple arrangement of areas with modal data points located on keypoints.

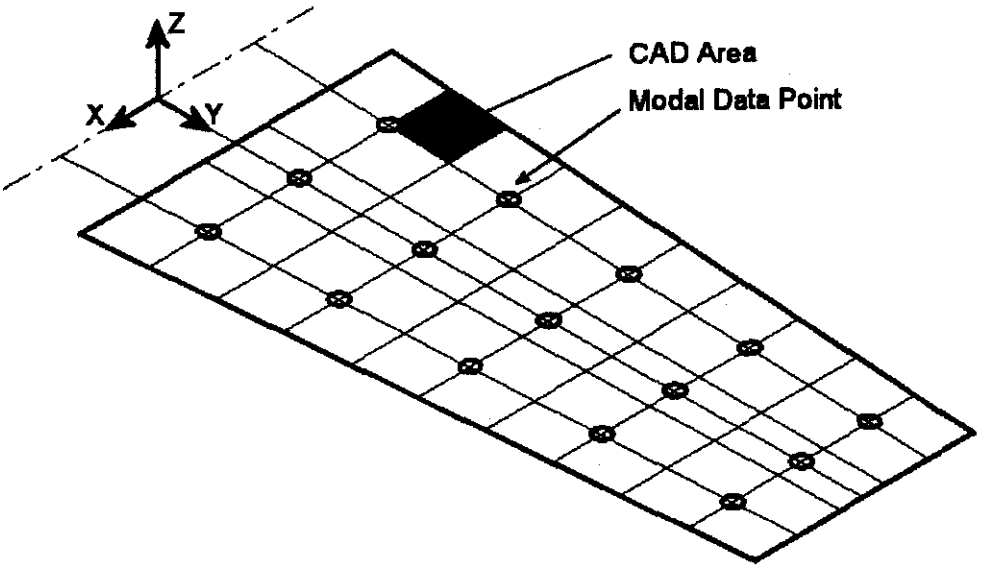

Figure 10: Modal Data Points

The complete CAD-model for the glider was generated taking these considerations into account. This produced a CAD-model which greatly simplified the generation of the finite element analysis (FEA) model, as will be shown in the next section.

3.2.2. FE modelling

Composite materials refer to a section containing more than one bonded material, each with its own structural properties. These materials are used extensively in the aircraft industry, mainly because of their high stiffness to weight ratio. Composites used for typical engineering applications are advanced fiber or laminated composites, such as fiberglass, carbon and Kevlar fibers.

The commercial FE-code, ANSYS, is capable of modelling composites with specialised layered elements. Once the model is built with these elements, one can perform any structural analysis. Section 2.3.2 provided some background on element types from which it was decided to use the SHELL99 element. Information regarding the lay-up definitions, substructuring and the complete FE-model will now be given.

3.2.2.1. Lay-up definition

The most important characteristic of composite materials is their layered configuration. Each layer may be made of a different orthotropic material and may have its principal directions oriented differently. For laminated composites, the fiber directions determine layer orientation. ANSYS uses a real constant table to specify these properties, which consist of:

- Material reference number (MAT)
- Layer orientation angle (THETA)
- Layer thickness (TK)

These properties were defined for each section of the complete glider that had a different lay-up. Figure 11 shows the front portion of the fuselage with each color representing a different lay-up schedule.

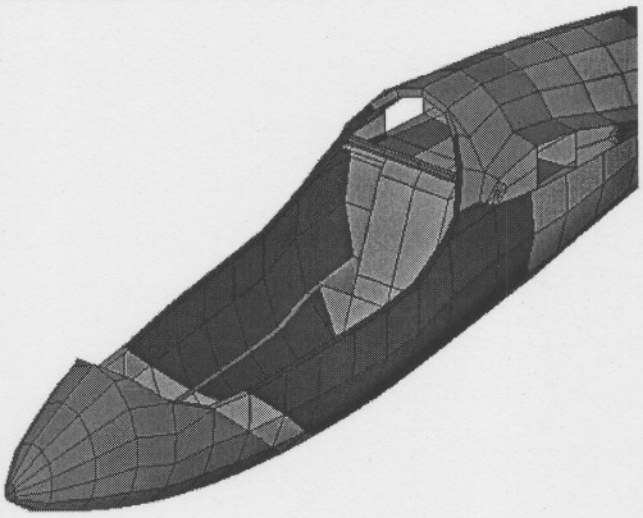

Figure 11: Front Fuselage FE-model

The complete glider consisted of nearly 200 real constant sets and used 35 local coordinate sets in order for it to be modelled as accurately as possible. The local coordinate sets are used as reference for the fiber orientation.

3.2.2.2. FE-models

The complete glider was modelled with 17635 elements and was further subdivided into components such as the wings, fuselage and tailplane. All the structures were modelled with SHELL99 elements, while rigid elements were used to connect the wings and tailplane to the fuselage. Figure 12 shows the rigid element connection between the front wing-pin and the fuselage. Similar connections were used to attach the tailplane to the fuselage.

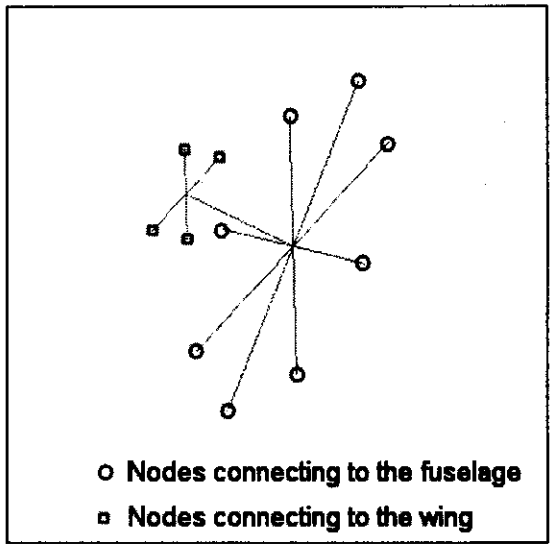

Figure 12: Rigid Element Connection

The control surfaces, consisting of the flaps, aileron and elevator were also attached to the lifting surfaces by means of rigid elements. This attachment method restricted all control surface movement and did not allow for deformation due to control system stiffness. This option was used because there was no measurable control system at the time of modelling. Once the first prototype has been completed, the stiffness of the control surfaces can be entered into the ANSYS model, whereafter the necessary control surface flutter scenario can also be investigated.

The complete FE-model took ±8 hours to solve on a Pentium 1.2 GHz processor, and with different configurations to analyse, that proved to be too long. In order to reduce the computer time it was decided to make use of substructuring. Substructuring is a procedure that condenses a group of elements into one element, represented as a matrix. This single element is called a super-element and can be used in an analysis as any other element. The only difference is that one first needs to create this super-element by performing a generation analysis on the desired selection of elements. The fuselage was selected as the ideal component to create into a substructure, while the connection nodes between the wings and tailplane were selected as Master Degrees of Freedom (MDOF). These nodes could then be used for attachments in any further

analysis. Figure 13 a) shows the substructured fuselage while the connection nodes on the fin can be seen in b).

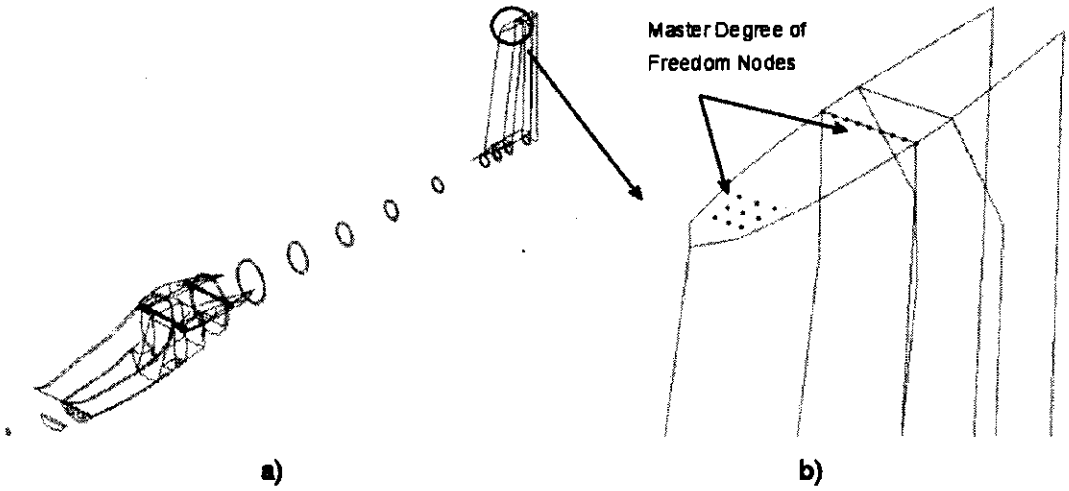

Figure 13: Substructured Fuselage

Modelling the glider in this way reduced the computer time to approximately one and a half hour per configuration, which was an acceptable time considering the complexity of the problem. The next step was to verify the model.

3.3. Verification

The importance of a verification process can be seen from a recent survey in which the modal analysis of a twisted cantilever beam had to be determined (Petyt, 1990). During this survey, several parties produced different results due to various modelling techniques, the elements used and the boundary conditions applied. The study therefore emphasised the need for a clear verification method.

For the purpose of this project, it has been decided to verify the glider-model with an independent analysis (also serving as a convergence test) as well as through experimental data. These procedures will now be discussed with regard to the stiffness and weight of the components.

3.3.1. Stiffness verification

3.3.1.1. Fuselage verification

Before the fuselage could be created as a sub-structure, it was verified by different team members by means of two independent FE-models. One model was created using SI-units while the other was created using the imperial units system. The imperial model was created since the input of the flutter code was restricted to imperial units. The SI-unit model consisted of 16913 elements while the imperial model consisted of 7337 elements. Both models were loaded in such a way as to determine the bending and torsional stiffness of the fuselage. Figures 14 a) and b) show the different loads that were used to during the verification. The deflection of the point (DP) as indicated in Figure 14 a) was used as reference.

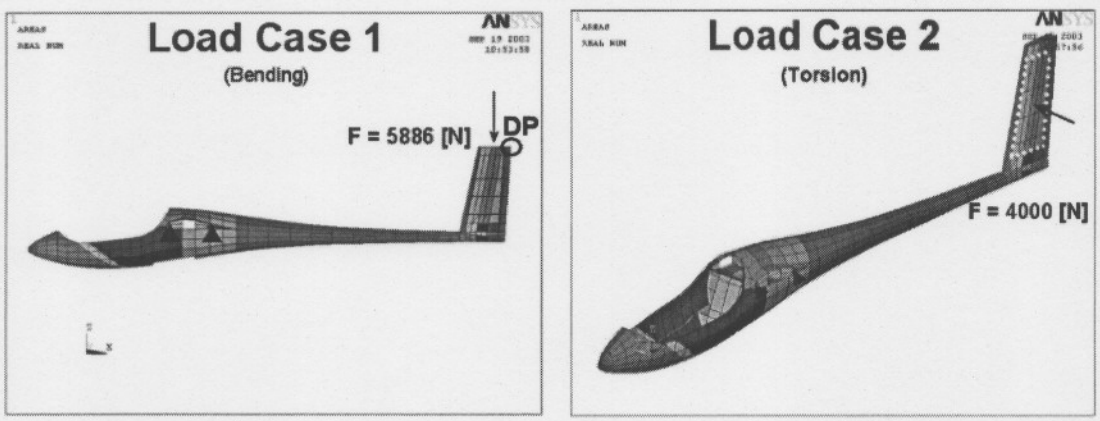

Figure 14: Fuselage Verification Loads

Comparing the vector displacements of the Deflection Point (DP) gave the following results:

Table 1: Fuselage Verification Results

	SI-model	IMP-model
Load Case 1 (Bending)	159.59 [mm]	**157.56 [mm]**
Load Case 2 (Torsion)	**172.69 [mm]**	**169.25 [mm]**

Table 1 shows a difference of less than 2% between the deflections of the two verifications models. With this close comparison it was accepted that the FE-model of the fuselage was a true representation of the real model, and that the slight difference between the results was largely due to the difference in the number of elements used.

The next verification made use of experimental data and will verify the actual stiffness of the composite materials.

3.3.1.2. Tailplane verification

The second verification process was an experimental data correlation and made use of a tailplane prototype. The tailplane was subjected to a simplified bending load, known as a whiffle tree loading. An illustration of this loading procedure as well as a photo of the actual test can be seen in figures 15 a) and b).

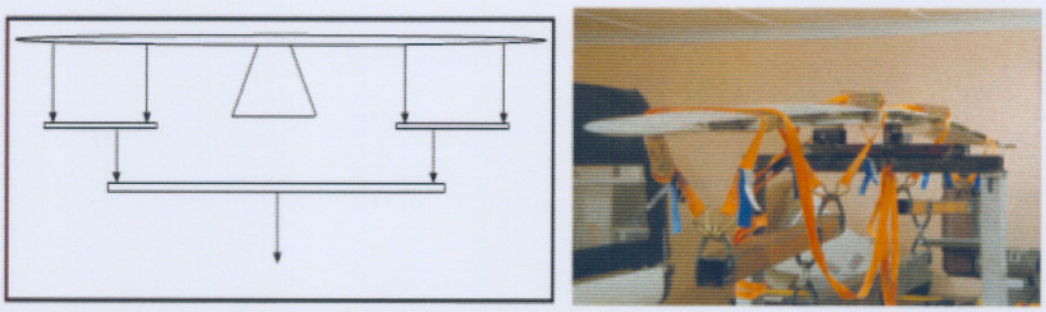

a) b)

Figure 15: Tailplane Testing

This load was chosen due to the fact that the bending displacements were among the easiest to measure. Applying these exact loads in the ANSYS model was also simplified because of this arrangement. Figure 16 shows the application of the appropriate loads (red arrows) on the ANSYS tailplane model, while the purple nodes were fixed in all degrees of freedom.

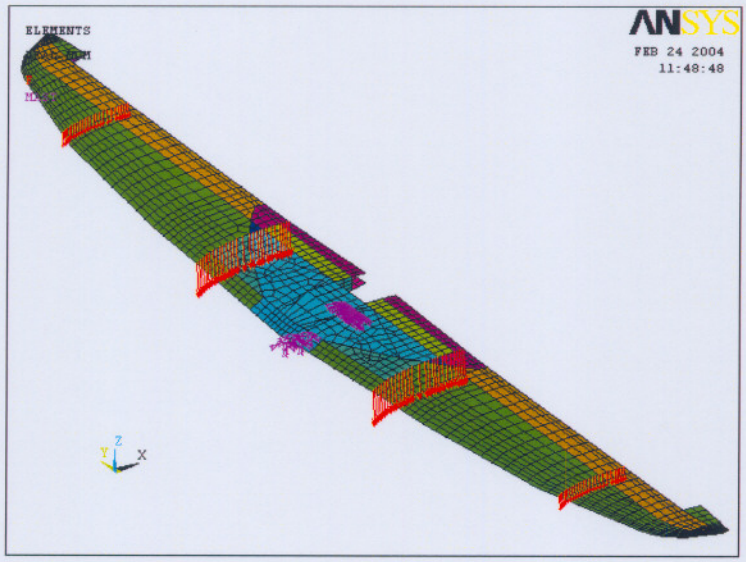

Figure 16: Tailplane FE-model

The tip deflection of both models was evaluated and the comparative results are summarised in table 2.

Table 2: Tailplane Comparative Results

	Tip Deflection [mm]
Actual Model	**84.5**
ANSYS Model	**83.6**

The results from table 2 provided a very good correlation and were accepted as the final verification with regards to the stiffness of the structure. From this verification it can be concluded that the stiffness of the different materials is realistically modelled and that no other stiffness test needs to be conducted for the rest of structure, as the same material properties are implemented everywhere.

The material properties that were used during this analysis were obtained by means of actual tests conducted with strain gauges in previous studies (Kühn, 2003). Appendix A1 provides a summary of them.

The final step in the verification process was now to ensure that the weight of each component was also accurately modelled, which will be discussed next.

3.3.2. Weight verification

The final verification process that needed to be completed was the updating of the FE-model mass to reflect realistic values. This was done by simply comparing the weight of the FE-models to those of existing or very similar components. The weight of the model was lower than that of the actual aircraft, due to the fact that no allowance was made for the paint, bonding glue, control linkage system, engine and payload. The ASH26 was chosen to be used as a comparative glider, since both it and the new glider would compete in the same 18m-class, and both use a similar lay-up schedule.

The following table sums up the masses of different components. These values represent a combination of similar existing components as well as certain weight-design limitations.

Table 3: Component Masses

Components	Mass [kg]
Fuselage	**151**
Pilot	**100**
Engine	**110**
Instruments	**7**
Single wing	**72**
Tailplane	**7.3**
Water (maximum)	**200**
Water (limited)	**92**

The weight of the fuselage FE-model was updated by simply increasing the densities of all the appropriate materials with a certain constant factor. This caused an even spread of the additional mass with no effect on the stiffness of the model. The additional masses in the fuselage, such as the pilot, engine and instruments were added by means of dummy layers. This refers to additional layers added to the specific real constant sets which had no stiffness, but did have the appropriate mass. Figure 17 shows the nose cone areas which were used for the additional 7 kg layer, representing the instrumentation weight. The pilot's weight where added to the seat while the engine were added to the engine bay cover.

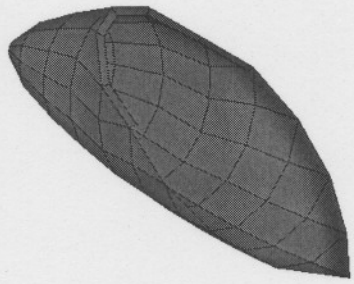

Figure 17: Areas where Instrumentation is added

The weight of the lifting surfaces was also added by means of a dummy layer. In this case every real constant set associated with that surface saw the addition of a layer with no stiffness and only mass. This seemed like the most appropriate way to add the extra weight required, which in practice would represent a combination of the epoxy, paint, gel coat and other manufacturing and finishing materials.

The final weight that need to be included in the model, was that of the water tanks in the wings. The first approach was to model these tanks as a series of mass-elements connected by a network of rigid elements. However, a test modal analysis concluded that the arrangement caused strange, natural frequencies within the wing. It was therefore decided to create an area that spread across the length of the wing. This area was given a layer with the same mass as the complete water tank, which solved the

problem of the mass-rigid network approach. Figure 18 shows a transparent view of the wing with the areas that were used as the water tanks.

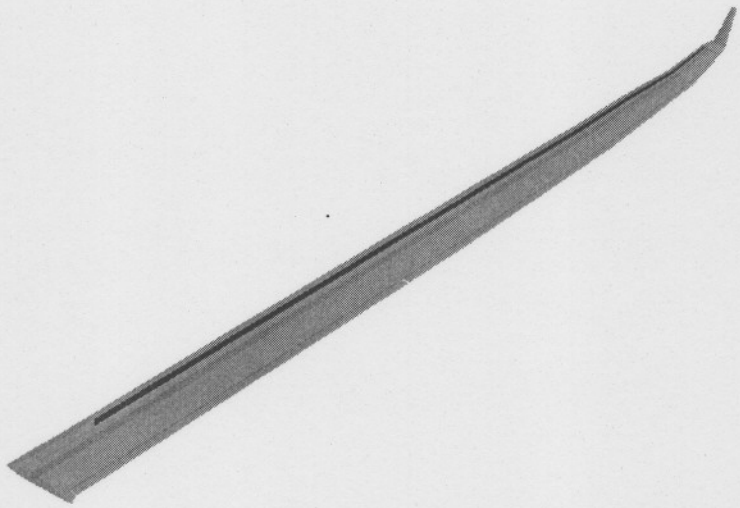

Figure 18: Water Tanks (Areas)

This area made use of an arbitrary material with a density that was calculated to provide the exact weight required. Other configurations, such as less water, could then easily be modelled by simply adjusting the density.

Updating the weights to the correct values was the last step of the verification process and prepared the model for the modal analysis.

3.4. Modal results

A modal analysis of the glider was performed for each of the different configurations. This analysis made use of the complete finite element model which consisted of the detail wings, tailplane and a substructured fuselage. These configurations corresponded to those used during the aerodynamic design and needed to be evaluated. An additional analysis was also performed to investigate the effect of modelling only one wing. This is followed by a comparison of the results.

3.4.1. Different configurations

The array of configurations that needed evaluation is summed up in table 4 and was merely a combination of components in order to keep the total weight under 600 kg. The basic configuration was dictated by the JAR-22 design specifications, while the specific configurations shown in table 4 were compiled by the development team.

Table 4: Glider Configurations

Configuration	Components				Total Weight
1	Fuselage	Wings	-	-	**400**
2	Fuselage	Wings	Engine	-	**500**
3	Fuselage	Wings	Engine	Water (92kg)	**600**
4	**Fuselage**	**Wings**	**-**	**Water (200kg)**	**600**

The difference between the first two configurations was the extra weight of the engine. This addition had no effect on the modal results of the lifting surfaces and will therefore not be included in the final results summary.

3.4.2. Results

3.4.2.1. Lifting Surfaces

The lifting surfaces consist of the wing as well as the tailplane, and are considered to be the most critical parts with regard to flutter. For this reason, it was necessary to determine the effect of modelling separate components as opposed to modeling the complete model. This investigation was proposed as varies flutter studies were conducted for single lifting surfaces. A single lifting surface would have the advantage of reducing the computational time to some extent, but could not have been done at the cost of inaccurate results. For this comparison it was chosen to analyze a single wing with no degrees of freedom boundary conditions being applied.

The first set of results provided a comparison between analyses of only the wings and a complete glider. Table 5 lists the modal results, which were solved for configuration 4, as this was the most critical one of them all.

Table 5: Comparison between One Wing and a Complete Glider

Configurations		
Complete Sailplane	**Wing Only**	Description
1.888	1.887	**1st Wing Bending (Symm)**
3.043	3.040	**1st Wing Bending (A-Symm**
6.048	6.047	**2nd Wing Bending (Symm)**
7.697	7.653	**2nd Wing Bending (A-Symm)**
12.119	12.119	**3rd Wing Bending (Symm)**
14.056	11.498	Wing Torsion (A-Symm)

A comparison between these two approaches showed that the bending frequencies of the wings stayed quite the same, regardless of the method. However, the torsion mode of the "wings alone" model showed less stiffness than the complete model. This was due to the fact that no fuselage-mass was connected to the wing pins. The complete model, with the wings connected at the wing pins, shows the added stiffness, and increased the torsion mode by 2.55 Hz. The effect of the fuselage on the modal analysis of the lifting surfaces was therefore regarded as a vital factor and was incorporated in all the analyses below.

The eigenvalues of the complete glider were then extracted for the first 30 natural frequencies. No displacements boundaries were applied, which caused the first 6 values to represent the translational and rotational natural frequencies about the three axis. These values were all almost zero, while the next 24 frequencies span from 0 Hz to about 50 Hz. These 24 modes included all the wing and tailplane modes. The tailplane was also subjected to a further modal analysis, which confirmed the first modal results.

Previous flutter scenarios (Hollmann, 1997:147) showed that the following modes where the most investigated ones among the main wings:

- 1st wing bending
- 2nd wing bending
- 3rd wing bending
- Aileron flapping together with first three bending modes
- Wing torsional mode

Apart from the aileron modes, all the others were obtained within the desired frequency band and are summed up in table 6. These results were taken from the complete model which consisted of a detailed wing and tailplane section, while the fuselage was substructured. Other modes that were omitted during this analysis included natural frequencies of components such as the water tank and other minor components. These modes / frequencies were regarded as non-relevant as the correct stiffness of these components were not included. The tailplane results are also presented in the following table.

Table 6: Lifting Surfaces Natural Frequencies

Configuration				
1 & 2 [Hz]	**3** [Hz]	**4** [Hz]	**Tailplane** [Hz]	Description
4.024	2.431	1.888	19.213	**1st wing bending (Symm)**
5.757	3.837	3.043	18.473	**1st wing bending (A-Symm)**
11.135	7.679	6.048		**2nd wing bending (Symm)**
14.538	9.684	7.697		**2nd wing bending (A-Symm)**
18.28	14.778	12.119		**3rd wing bending (Symm)**
23.856	**16.67**	**14.056**		**Wing torsion**

These modal results compared well with the results from other gliders and a comparison between the extracted modes sequence can be seen in the next table.

Table 7: Comparative modal results (Hollmann, 1997)

	Modes Extracted		
	1st wing bending	**2nd wing bending**	3rd wing bending
JS1 (this study)	2.431	7.679	**14.778**
Cygnet	3.924	13.058	**29.05**
ASH26	**2.0**	**Not available**	**Not available**

Figure 19 shows some of the mode shape displacements associated with the natural frequencies of configuration 4 of the complete model with the substructured fuselage. These plots used a displacement scaling factor of 4.5 in order to distinguish clearly between the different modes, while the substructured fuselage element was hided in some instances to more clearly see the results. The tailplane elements were not selected for this figure in order to obtain a complete spectrum for the wings.

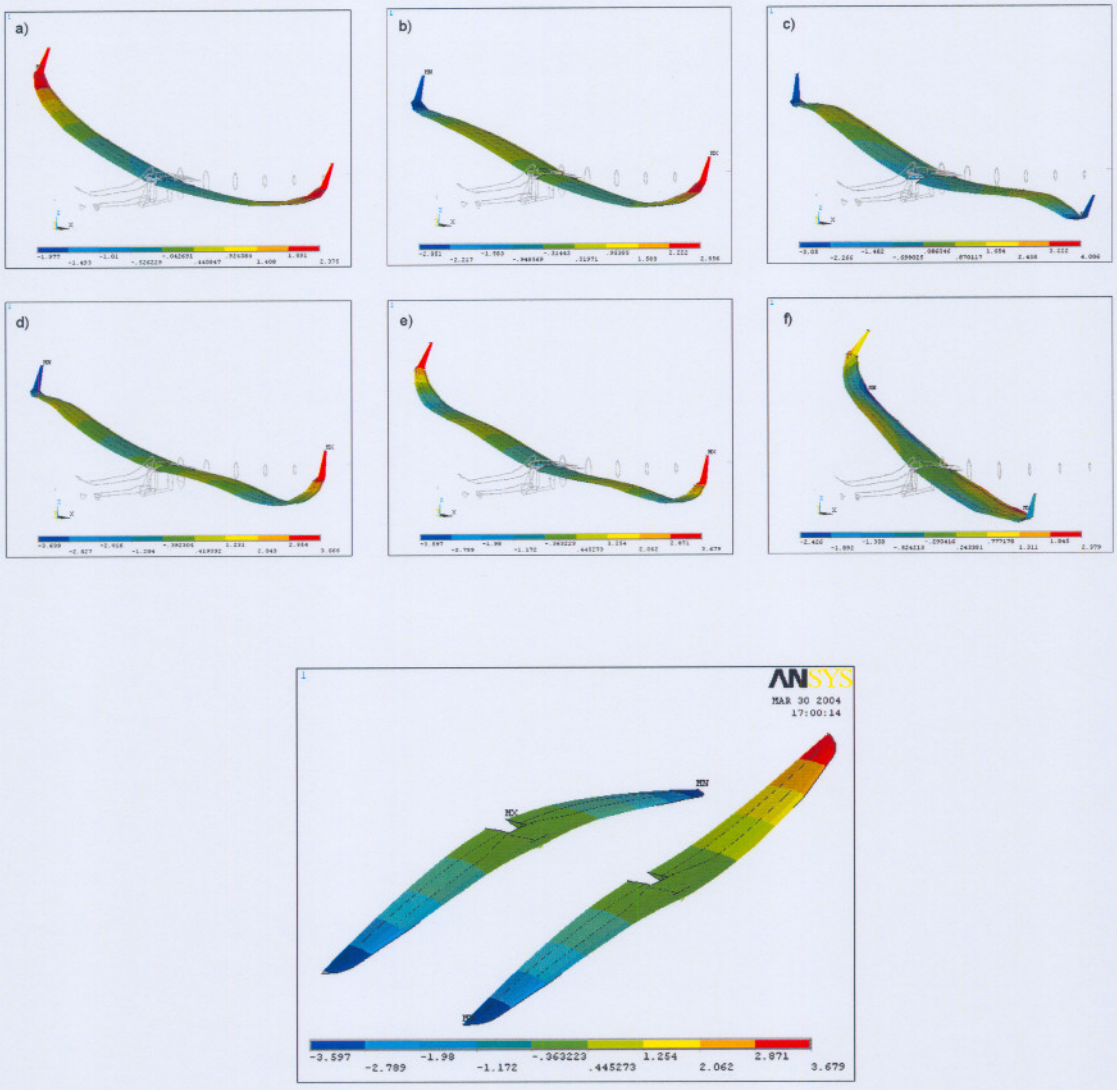

Figure 19: Mode shapes

The final results to be presented are those of the fuselage together with the fin.

3.4.2.2. Fuselage – Fin Structure

The fuselage of an 18m-class glider is a long slender body with natural frequencies well in range of the flutter boundaries. The fact that the fin, an aerodynamical component, is attached to the structure, makes it necessary to perform a flutter analysis on this structure. In order to perform this study, it is necessary first to calculate the modal data associated with its natural frequencies.

The model that was used consisted of the fuselage with a substructured tailplane. This substructured tailplane was used to simulate its effect on the fin, while not solving the tailplane again. Figure 20 shows this model. This model was analyzed with no constraints on the fuselage.

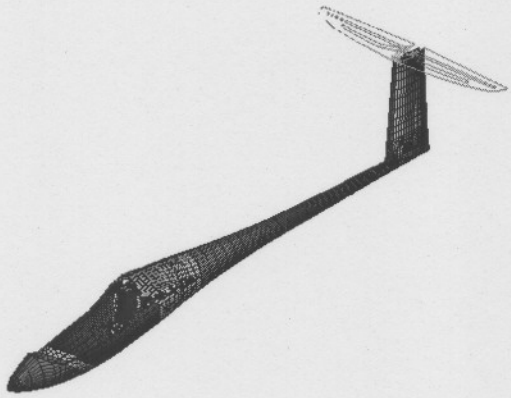

Figure 20: Fuselage - Fin model

The results from this analysis concluded that the fuselage and fin bending were within the frequency band of the lifting surfaces. The fin bending was obtained at 11.66 Hz while the fuselage displayed this behaviour at 14.735 Hz. Figures 21 a) and b) show the deformation of these two mode shapes.

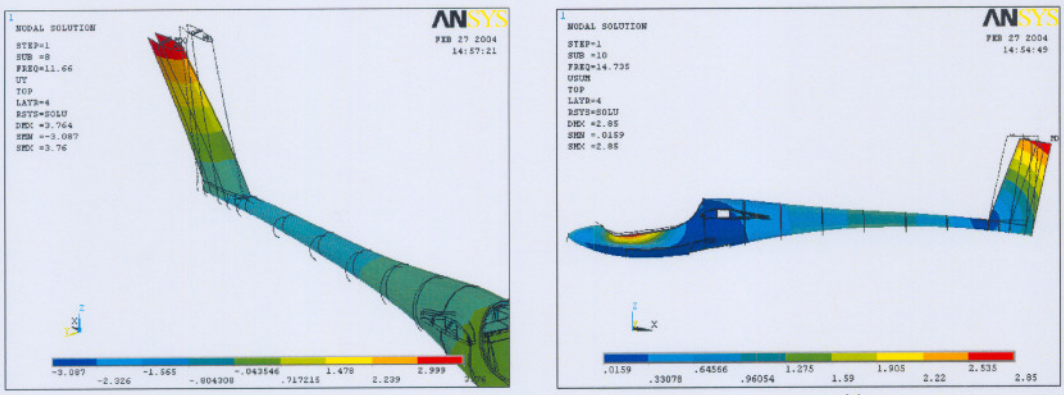

a) b)

Figure 21: a) Fin Bending **b) Fuselage Bending**

The fin bending resulted in displacements of up to almost 4 inches while the fuselage maximum value was 2.75 inches. From these results, it was obvious that the flutter analysis also needed to be conducted on the T-tail configuration.

3.5. Summary

The modal analysis of the complete 18m-class glider has been performed with the aid of FE modelling. The process made use of the commercially available software code ANSYS. In order to perform the analysis, it was necessary to create a very detailed CAD-model with the following in mind:

- Most effective way of modelling surfaces;
- Preparing the CAD-model for different lay-up schedules; and
- Preparing the model with the data extraction points in mind.

This was all done successfully and greatly facilitated the final creation of the FE-model. The complete FE-model was then verified by means of independent modelling as well as with experimental testing. Both the FE-model and experimental verifications showed deviations of no more than 2% and were accepted as a good correlation. The verifications were also used for updating the stiffness and mass of the model for the final modal analysis.

The modal analysis was then performed for four different configurations. The configurations represented combinations of components in order to limit the maximum weight to 600 kg. The results from each of the configurations were obtained within the desired frequency band of 0 – 50 Hz and consisted of

- 1st wing bending
- 2nd wing bending
- 3rd wing bending
- Wing torsional mode
- Tailplane, 1st bending and
- Fin bending.

The addition of the fin bending results emphasised the need for the flutter analysis to also extend to the T-tail configuration.

4 Flutter Analysis

4.1. Introduction

In this section the flutter analysis of the JS1 sailplane will be discussed. The flutter analysis is the final part of this study that started with the generation of the CAD-model, and then proceeded to the calculation of the modal analysis. The modal displacements associated with each natural frequency will now be used in a commercial flutter code SAF (Subsonic Aerodynamic Flutter) to determine the critical flutter speed of the aircraft. This code implements the doublet lattice method, which can be regarded as one of the best tools for analysing multiple surfaces (Wilkinson et al, 1975). It also provides a choice between the K and pK solution method, with the latter being the more appropriate.

The results from this analysis will then be presented as plots of damping and frequency vs. true airspeed. The airspeed will be indicated in knots, due to the fact that SAF uses only imperial units. In general, flutter can be described as either 'merging frequency flutter' or 'single degree of freedom flutter'. Merging flutter occurs when two natural frequencies approach each other, with either one becoming unstable. The instability is shown by the damping graph crossing the zero line and is illustrated in figure 22 a). Single degree of freedom flutter is when the damping of a single mode becomes positive.

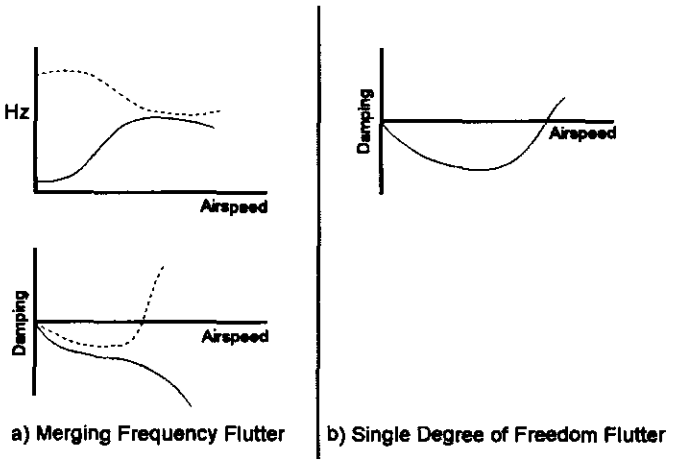

Figure 22: Different types of flutter

Next, both these trends will be investigated to determine whether the aircraft displays sufficient stability in the desired velocity range up to 390 km/h.

The following section will now first provide information regarding the preparation of the flutter models, whereafter the results will be presented.

4.2. *Input Preparation*

SAF uses a text input file which contains all the necessary information to conduct a flutter analysis. This information includes the geometric description by means of a panel model, the modal data as well as all the necessary flutter settings. This section will now provide an overview of the panel model that was used in this analysis.

Panel Creation

The first step was to subdivide all the lifting surfaces into panels. These panels are defined by a local coordinate system and were restricted to trapeziums. For the purpose of this project it was decided to create a panel model with as much detail as possible. Simplified models have been used on glider wings, but resulted in a more conservative analysis (Hollmann, 1997:31). Figure 23 shows the panel model for the complete glider.

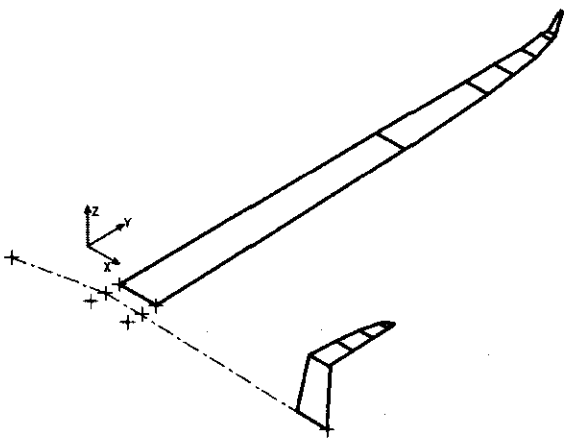

Figure 23: Panel Model

The model consisted of 12 panels and was further subdivided into doublet lattice elements from which the interaction between the free-stream and structure was calculated. Figure 24 shows the distribution of elements on some of the wing panels.

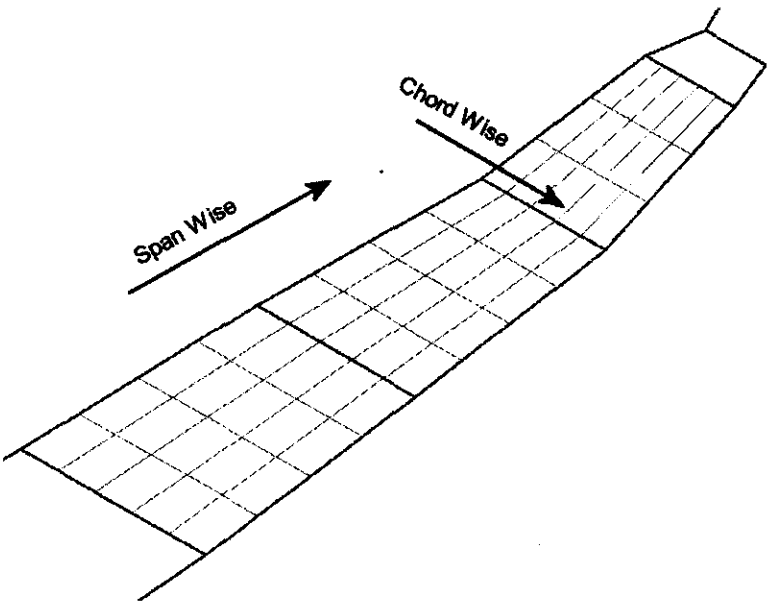

Figure 24: Doublet Lattice Elements

Modal Points

The final preparation was the definition of the modal points. These points were the same as those described in section 3.2.1, but connected by straight lines. These lines were used for interpolating and extrapolating the modal data to other parts of the lifting surfaces. The tailplane modal data points can be seen in the next figure.

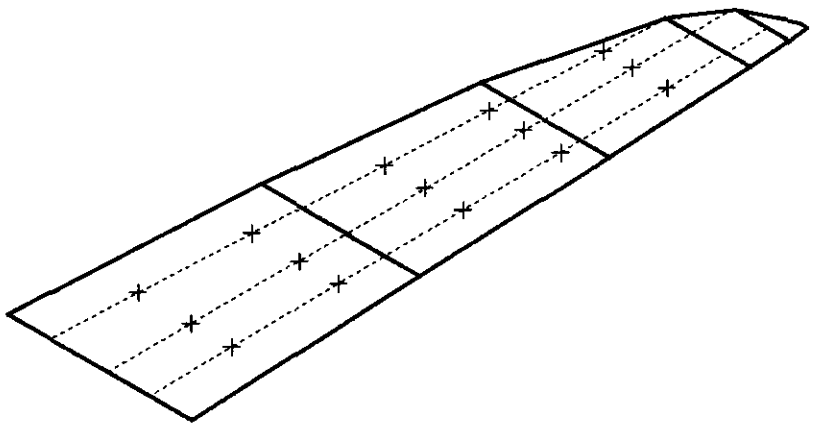

Figure 25: Tailplane Modal Points

The final text files needed the modal data for each point, natural frequency and configuration. The process of adding these values to text files seemed too time-consuming and was implemented into an EXCEL spreadsheet. The spreadsheet made use of ANSYS nodal results output files, and converted these to the desired SAF input format. This tool ensured a minimum preparation time and additional features such as analysis and panel information could easily be manipulated. Appendix A2 includes some of the final input files that were used.

4.3. Flutter results

The flutter results were computed for each of the four configurations of the wing and tailplane model, as well as a separate analysis for the fin. This fin analysis made use of the fin-results as described in chapter 3 for the fuselage with substructure tailplane analysis. These analyses were performed separately for symmetric and asymmetrical modes. Structural damping of 3% was applied throughout the entire analysis and might be updated once a GVT has been performed.

The analysis was also performed for altitudes, ranging from sea level to 25 000 feet. The outcome was a series of graphs for different configurations and altitudes which all displayed a similar trend. Because of the high number of plots, it was decided to

recognise a general pattern among the plots and provide an interpretive analysis, with the remaining graphs being shown in appendix A3. The first results that will be presented are those of configurations 1 & 2.

The 1st and 2nd asymmetric bending modes showed signs of merging frequency flutter in the region of 300 knots (at all altitudes), and can be seen in figure 26. This value is about 70% higher than the limit of 209.9 knots ($1.2V_D$), and is therefore of no concern. From figure 27 it can be concluded that each mode has sufficient damping and that both modes will remain stable.

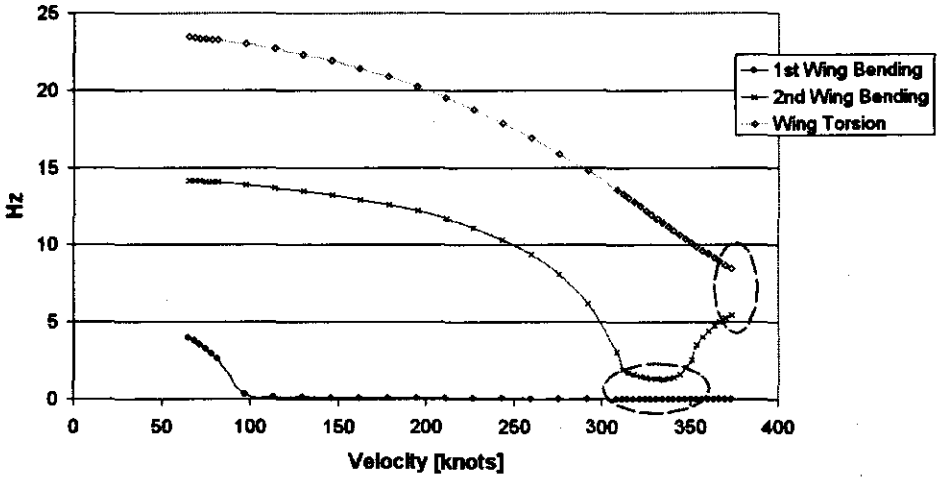

Figure 26: V-Hz graph (Configuration 2, Asymmetric)

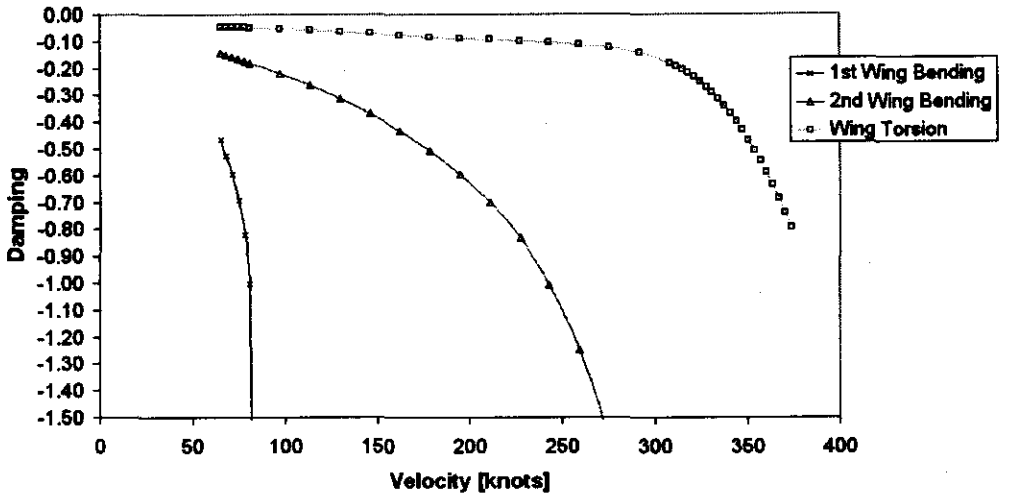

Figure 27: V-g graph (Configuration 2, Asymmetric)

The symmetric modes of configurations 1&2 showed no tendency towards merging flutter while the damping also remained negative. The graphs will not be presented as they are very similar to those seen in figure 29.

Configuration 3 saw the addition of 92 kg of water, which made the glider more susceptible to flutter. The V-g graphs of both symmetric and asymmetric modes indicated a possibility of merging flutter. This tendency shifted to about 250 knots and is due to the weight of the extra water. Figures 28 and 29 illustrate this behaviour.

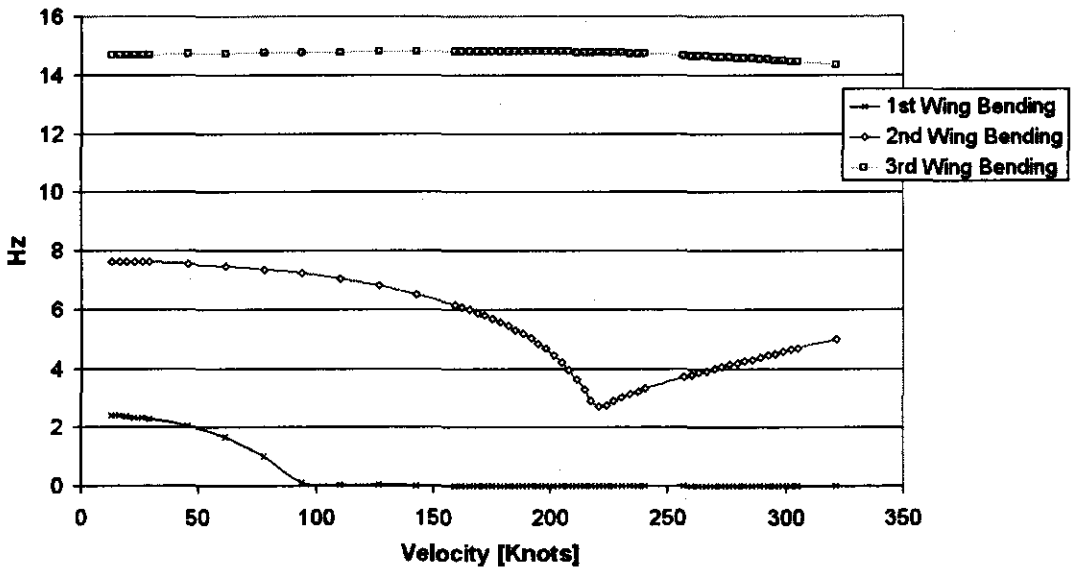

Figure 28: V-Hz graph (Configuration 3, Symmetric)

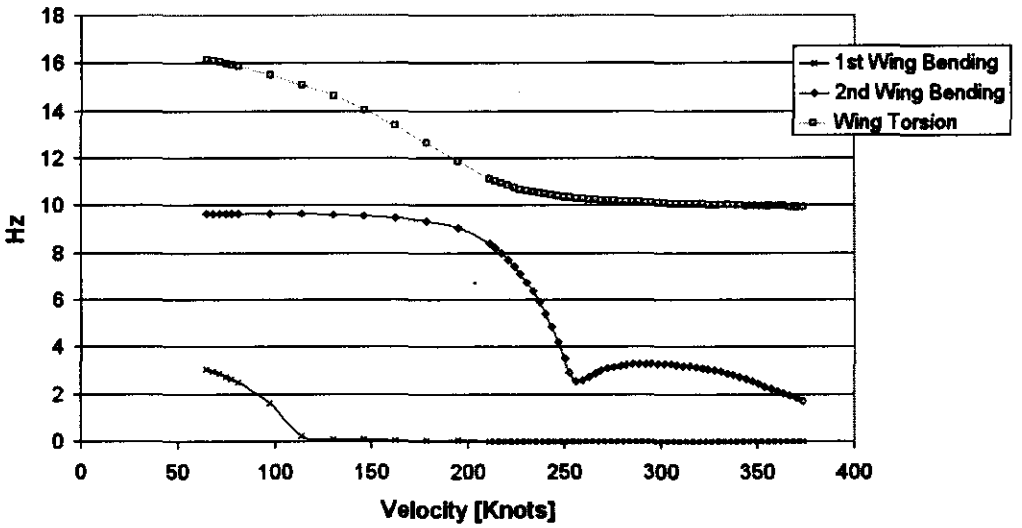

Figure 29: V-Hz graph (Configuration 3, Asymmetric)

The damping of these modes again indicated stability over the entire tested spectrum. Figure 30 shows the damping trend of the symmetrical modes for configuration 3. The asymmetrical modes differ very little and also showed stability over the entire velocity range.

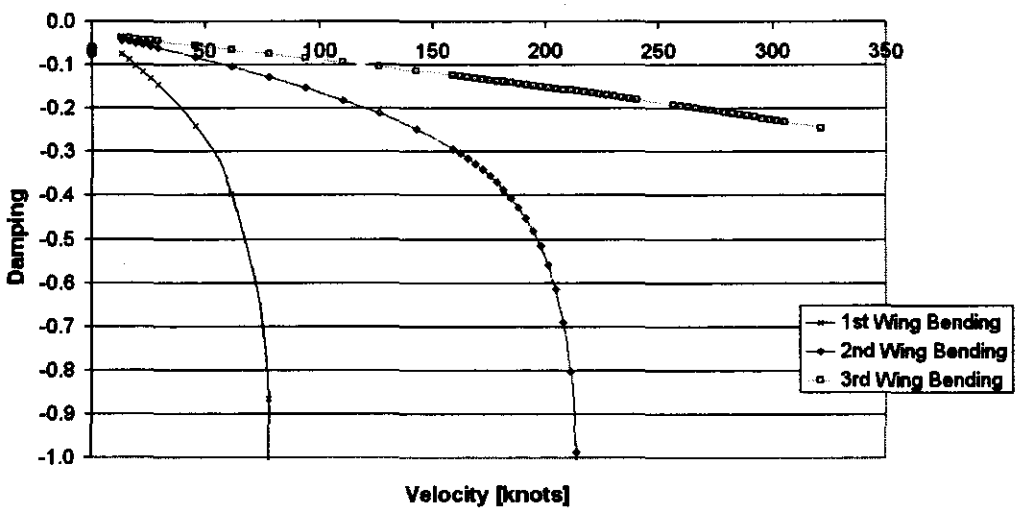

Figure 30: V-g graph (Configuration 3, Symmetric)

The final results concerning the wings are those of configuration 4. This configuration had the full load of water in the wings, which added 200 kg to the total weight. The addition of this extra weight lowered the natural frequencies by almost 50%. From the frequencies plots, figure 31, it can be observed that the tendency of merging flutter still continued. This occurrence was now between the 1st and 2nd symmetric bending modes and in the region of 170 knots. Figure 31 also illustrates that this appearance seemed more severe than the previous cases.

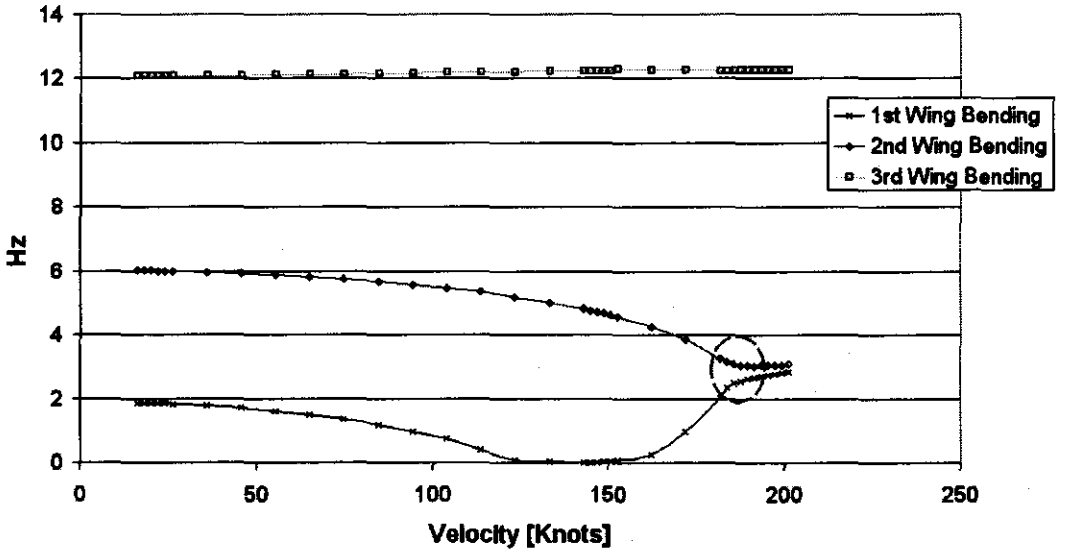

Figure 31: V-Hz graph (Configuration 4, Symmetric)

The damping of the symmetric modes indicated that all the modes remained stable (Figure 32). The two modes involved in the merging flutter scenario also showed a rapid increase in damping values (thus more negative), which minimised the possibility of flutter.

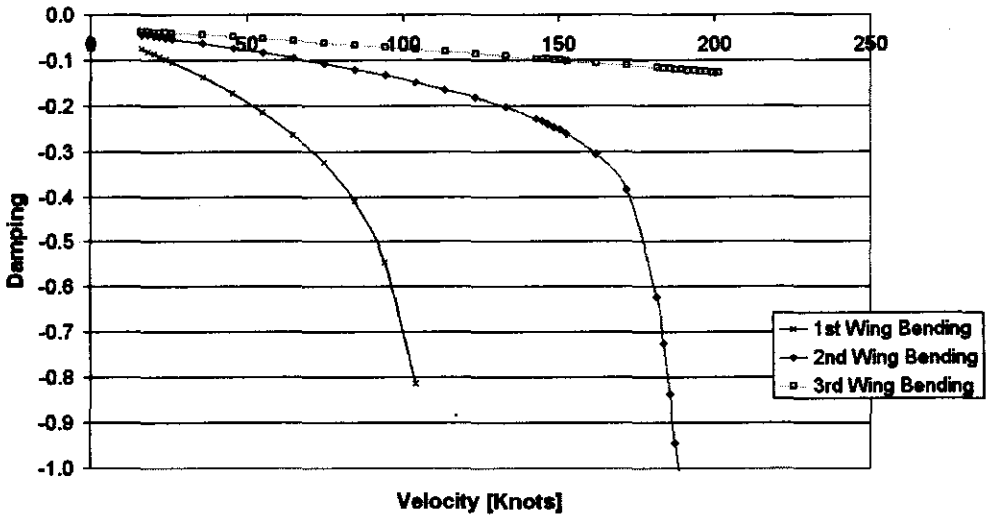

Figure 32: V-g graph (Configuration 4, Symmetric)

The fin and tailplane configurations were also analysed at different altitudes and again displayed similar trends over the complete result set. The first figure shows the frequencies of the appropriate modes, while the damping graph indicates the stability of the rear structure.

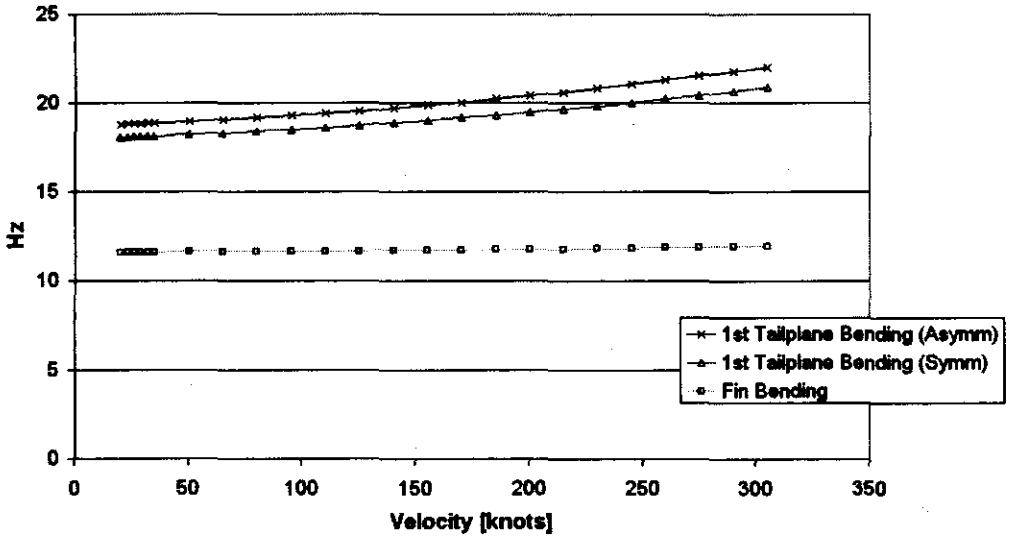

Figure 33: V-Hz graph (Tailplane Configuration)

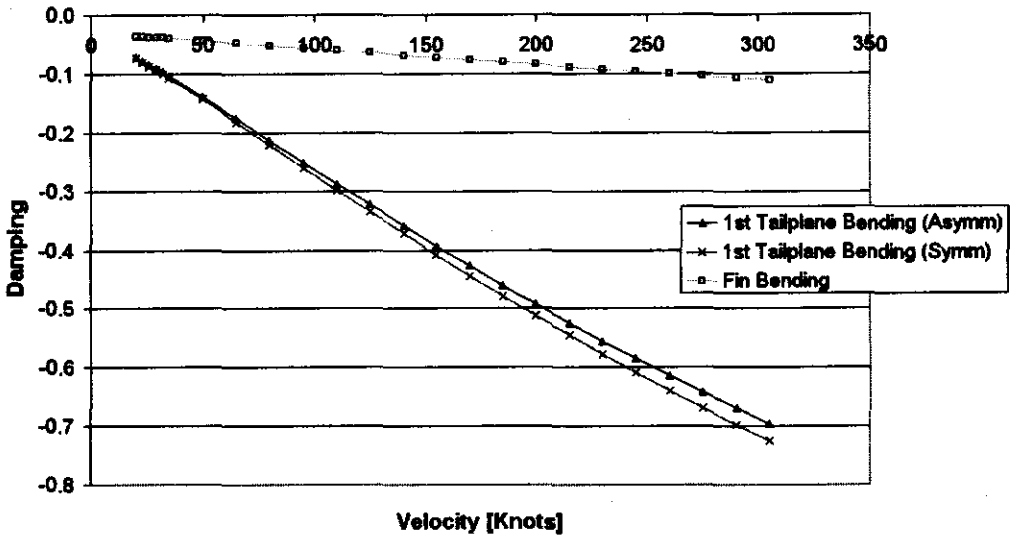

Figure 34: V-g graph (Tailplane Configuration)

These graphs also indicated no flutter in the tested region and showed that adequate damping was available for all modes.

4.4. Summary

The flutter analysis of the JS1 18m glider was performed with the commercially available code, SAF. This code makes use of the doublet lattice method while the solution was obtained with the pK algorithm.

A detailed panel-model of the glider was constructed, which was used to evaluate the flutter characteristics of the main natural modes. These modes included the 1st, 2nd and 3rd bending of the wings as well as asymmetric torsion. The T-tail configuration was also investigated.

The analysis made use of 3% structural damping throughout the structure and was conducted up to 25 000 ft in altitude. Because four configurations needed testing at different altitudes, there was a large number of graphs. The results all showed a similar trend and could be regarded as near cases of "merging frequency flutter" and "single

degree of freedom flutter". Although some configurations were more suspect to flutter than other, the damping-graphs indicated stability over the full spectrum.

This theoretic analysis therefore concluded that the JS1 glider is free from main-mode flutter up to 1.2 times the designed velocity (V_D) of 324 km/h and up to 25 000 ft.

5. Conclusion

5.1. Conclusion

In this study, the flutter characteristics of the JS1 18m class glider were investigated. This preliminary theoretic flutter analysis was restricted to the main lifting surfaces and is necessary for the certification of this glider. The results from the flutter analysis will also be used during its first flight tests, in order to approach flutter boundaries carefully. The complete study was divided into the modal analysis procedure and the flutter analysis.

The modal analysis was done by means of finite element modelling with the commercial code ANSYS. A complete FE-model of the glider was created, incorporating techniques such as substructuring. This approach was selected because a complete aircraft had not yet been completed at the time of this study. This FE-model made use of a detailed recreated CAD-model which took account of the following:

- Optimal surface definition for FE-modelling
- Preparation of CAD-model for different lay-up schedules
- And modal data extraction points

Verification of the model was conducted through independent FE-analysis as well as comparative experimental results. Both verification methods resulted in correlations within 2% and were accepted as satisfactory. These verification methods were also used to update the FE-model to be as accurate as possible.

The final modal analysis was obtained for four different configurations. The results from each configuration were obtained within the frequency band of 0 – 50 Hz and consisted of the following symmetrical and asymmetrical modes:

- 1st wing bending
- 2nd wing bending

- 3rd wing bending
- Wing torsional mode
- Tailplane, 1st bending and
- Fin bending.

These results, together with the associated modal displacements, were then used as the main input for the flutter analysis. The flutter analysis was conducted with the commercial code SAF (Subsonic Aviation Flutter), which implemented the doublet lattice method. This analysis was also performed for each of the different configurations and at altitudes ranging from sea level to 25 000 ft.

The results from the flutter analysis were presented as graphs of damping and natural frequency versus airspeed. From these graphs it could be concluded that there was a slight overall tendency towards "merging frequency flutter". The damping graphs, however, indicated stability over the entire tested region, which ensured that the glider was free from main mode flutter up to 388.8 km/h ($1.2 \cdot V_D$) and 25 000 ft.

5.2. *Recommendations for further studies*

In order to apply for certification of this newly designed JS1 18m glider, a complete flutter analysis has to be performed. In this preliminary study, the flutter analysis excluded the control surfaces. A further study, which includes all control surfaces, must therefore be performed before the first flight test. Measured control surface stiffnesses should be used in this study, while a ground vibration test will also serve to validate the results from this study. This study could also include a more detailed flutter analysis of the T-tail configuration.

An additional project which could further assist the flutter analysis process is a graphical user interface (GUI) for the commercial code SAF. This will eliminate the time-consuming procedure of creating text input files by hand and would drastically reduce the preparation time.

A1: Material Properties

Material Description	E_x	E_y	E_z	G_{xy}	Pr_{xy}	Rho
	[Mpa]					*[kg/m^3]*
Bi-directional Glass	22500	22500	1000	4200	0.28	2527
Uni-directional Glass	32000	8000	1000	3200	0.25	2527
Bi-directional Kevlar	38000	38000	1000	2200	0.15	1433
Uni-directional Kevlar	60000	5000	1000	1500	0.34	1433
Bi-directional Carbon	55000	55000	1000	4000	0.08	1892
Uni-directional Carbon	96000	8000	1000	3000	0.2	1892
Carbon Rovings	103000	7000	7000	3000	0.2	1892
Foam	60	60	60	-	0.3	83
Wood	20000	20000	20000	-	0.3	498

1/2

```
 1
Flutter analysis of JS1 sailplane
Multi panel with  245  elements
No control surfaces
P-K flutter type
 3  vibration modes: Config 2 Symm
mach=0.01
-1   3   1   6   5   0   0   0   0   0
 1   0   1   0   0   1   0   0   1   0
 1   0   0   1   0   0   0   0   0   0
 0   0   0   0   0   0   1
 30
-0.56306  -0.51576  -0.42944  -0.14204   0.22778   0.78379   1.3558
 2.2309   3.3653   4.1785  -0.74663  -0.68172  -0.5909  -0.32641
 0.090188   0.64749   1.2264   2.1262   3.2735   4.1024  -0.94648
-0.88921  -0.88921  -0.771  -0.47675  -0.047734   0.53027   1.1211
 3.186   4.0177
-0.99156  -0.82237  -0.50485   0.23768   1.0058   1.6975   1.9949
 1.7193   0.24116  -1.4772  -1.2469  -1.0511  -0.72818   0.077297
 0.93344   1.5205   1.8382   1.5574   0.092896  -1.6284  -1.5309
-1.3515  -1.3515  -0.98236  -0.12955   0.75811   1.3812   1.6924
-0.069317  -1.7987
-0.27909  -0.10949   0.13732   0.52634   0.71547   0.40347  -0.29634
-1.366  -1.644  -0.83758  -1.0576  -0.81223  -0.52245   0.40425
 0.54797  -0.12154  -0.78407  -1.8155  -2.0424  -1.1425  -1.9113
-1.6804  -1.6804  -1.2378  -0.2479   0.042355  -0.53044  -1.2035
-2.4377  -1.5466
 1
 1   1   144   2   2   144   3   3   144
 4.024   11.135   18.28
 15.524   0.276
 20   20   15
 0.02   0.5   1   5   10   15   50
 0.03
 0.5  -0.5   600   30
 1   0.8237   0.6696   0.5361   0.4216
 31.048   1
 1   7   0   735   0   0   1
**Panel 1 (100 elements)
 0   0   0   1.943
-15.524   15.524  -11.455   12.711   12.441   224.163
 1.146   8.329   21   6   0
 0   0.2   0.4   0.6   0.8   1
 0   0.05   0.1   0.15   0.2   0.25
 0.3   0.35   0.4   0.45   0.5   0.55
 0.6   0.65   0.7   0.75   0.8   0.85
 0.9   0.95   1
**Panel 2 (40 elements)
 0   0   0   4.213
-11.455   12.711  -6.778   12.042   224.163   295.024
 8.329   13.549   9   6   0
 0   0.2   0.4   0.6   0.8   1
 0   0.125   0.25   0.375   0.5   0.625
 0.75   0.875   1
**Panel 3 (20 elements)
 0   0   0   8.435
-6.778   12.042  -4.354   11.853   295.024   316.583
 13.549   16.746   5   6   0
 0   0.2   0.4   0.6   0.8   1
 0   0.25   0.5   0.75   1
**Panel 4 (20 elements)
 0   0   0   8.315
-4.354   11.853  -1.068   11.506   316.583   336.31
 16.746   19.629   5   6   0
 0   0.2   0.4   0.6   0.8   1
 0   0.25   0.5   0.75   1
```

2/2

```
**Panel 5 (15 elements)
 0   0   0   23.895
-1.068   11.506   2.339   11.378   336.31   349.577
 19.629   25.507   4   6   0
 0   0.2   0.4   0.6   0.8   1
 0   0.33333   0.666667   1
**Panel 6 (10 elements)
 0   0   0   34.324
 2.339   11.378   5.557   11.638   349.577   352.535
 25.507   27.85   3   6   0
 0   0.2   0.4   0.6   0.8   1
 0   0.5   1
**Panel 7 (40 elements)
 0   0   0   84.928
 5.557   11.638   13.667   15.832   352.535   354.141
 27.85   45.949   9   6   0
 0   0.2   0.4   0.6   0.8   1
 0   0.125   0.25   0.375   0.5   0.625
 0.75   0.875   1
 1   0   0   0   0   0
 1   245   0
F  245   0
 3   0   1   1
 10  -11.508   0  -1.524   354
 26.36   52.07   79.99   121.81   159.06   195   224.16   259.69
 295.09   316.58
 10  -0.159   0   3.949   354
 26.36   52.07   79.99   121.81   159.06   195   224.16   259.69
 295.09   316.58
 10   11.698   0   9.882   354
 26.36   52.07   79.99   121.81   159.06   195   224.16   259.69
 295.09   316.58
 0
0
```

1/2

```
 1
Flutter analysis of JS1 sailplane
Multi panel with  245  elements
No control surfaces
P-K flutter type
 3  vibration modes: Config 2 A-Symm
mach=1.2xVd
-1   3   1   6   5   0   0   0   0   0
 1   0   1   0   0   1   0   0   1   0
 1   0   0   1   0   0   0   0   0   0
 0   0   0   0   0   0   1
 30
-0.21449  -0.40382  -0.58108  -0.70043  -0.65039  -0.3031   0.20742
 1.2036   2.7134   3.9141  -0.2164  -0.40812  -0.58991  -0.79737
-0.69231  -0.3078   0.20108   1.2119   2.7226   3.9286  -0.22116
-0.41853  -0.41853  -0.60568  -0.79903  -0.70363  -0.31931   0.203
 2.7402   3.9506
-0.2021  -0.33402  -0.40338  -0.050192   0.44511   1.3998   2.2089
 2.7103   1.7099  -0.13921  -0.22278  -0.38481  -0.49721  -0.618
 0.2324   1.2517   2.0802   2.5786   1.5856  -0.28698  -0.25663
-0.46514  -0.46514  -0.61978  -0.68004   0.088094   1.1256   1.9605
 1.4463  -0.43407
 0.52518   0.98481   1.267   1.2534   1.1551   0.77185   0.94449
 1.0802   1.1461   0.84929   0.42899   0.77061   0.92338   0.62702
-0.68872  -0.23223  -0.065072   0.15869   0.25985   0.075723   0.32508
 0.547   0.547   0.63807  -0.077208  -1.4713  -1.0394  -0.89073
-0.61899  -0.83651
 1
 1   1   144   2   2   144   3   3   144
 5.757   14.538   23.856
 15.524   0.276
 20   100   25
 0.02   0.5   1   5   10   15   50
 0.03
 0.5  -0.5   600   30
 1   0.8237   0.6696   0.5361   0.4216
 31.048   1
-1   7   0   735   0   0   1
**Panel 1 (100 elements)
 0   0   0   1.943
-15.524   15.524  -11.455   12.711   12.441   224.163
 1.146   8.329   21   6   0
 0   0.2   0.4   0.6   0.8   1
 0   0.05   0.1   0.15   0.2   0.25
 0.3   0.35   0.4   0.45   0.5   0.55
 0.6   0.65   0.7   0.75   0.8   0.85
 0.9   0.95   1
**Panel 2 (40 elements)
 0   0   0   4.213
-11.455   12.711  -6.778   12.042   224.163   295.024
 8.329   13.549   9   6   0
 0   0.2   0.4   0.6   0.8   1
 0   0.125   0.25   0.375   0.5   0.625
 0.75   0.875   1
**Panel 3 (20 elements)
 0   0   0   8.435
-6.778   12.042  -4.354   11.853   295.024   316.583
 13.549   16.746   5   6   0
 0   0.2   0.4   0.6   0.8   1
 0   0.25   0.5   0.75   1
**Panel 4 (20 elements)
 0   0   0   8.315
-4.354   11.853  -1.068   11.506   316.583   336.31
 16.746   19.629   5   6   0
 0   0.2   0.4   0.6   0.8   1
 0   0.25   0.5   0.75   1
**Panel 5 (15 elements)
 0   0   0   23.895
```

2/2

```
**Panel 5 (15 elements)
 0   0   0   23.895
-1.068   11.506   2.339   11.378   336.31   349.577
 19.629   25.507   4   6   0
 0   0.2   0.4   0.6   0.8   1
 0   0.33333   0.666667   1
**Panel 6 (10 elements)
 0   0   0   34.324
 2.339   11.378   5.557   11.638   349.577   352.535
 25.507   27.85   3   6   0
 0   0.2   0.4   0.6   0.8   1
 0   0.5   1
**Panel 7 (40 elements)
 0   0   0   84.928
 5.557   11.638   13.667   15.832   352.535   354.141
 27.85   45.949   9   6   0
 0   0.2   0.4   0.6   0.8   1
 0   0.125   0.25   0.375   0.5   0.625
 0.75   0.875   1
 1   0   0   0   0   0
 1   245   0
F  245   0
 3   0   1   1
 10  -11.508   0  -1.524   354
 26.36   52.07   79.99   121.81   159.06   195   224.16   259.69
 295.09   316.58
 10  -0.159   0   3.949   354
 26.36   52.07   79.99   121.81   159.06   195   224.16   259.69
 295.09   316.58
 10   11.698   0   9.882   354
 26.36   52.07   79.99   121.81   159.06   195   224.16   259.69
 295.09   316.58
 0
```

```
 1
Flutter analysis of JS1 sailplane: Fin
Multi panel with  155  elements
No control surfaces
P-K flutter type
 1  vibration modes: A_Symm
mach=1.2xVd
-1   1   1   6   5   0   0   0   0   0
 1   0   1   0   0   1   0   0   1   0
 1   0   0   1   0   0   0   0   0   0
 0   0   0   0   0   0   1
 21
-0.46743  -0.094746   0.2918   0.70813   1.1495   1.609   2.2265
-0.32342   0.045379   0.43011   0.84142   1.2747   1.725   2.3322
-0.208   0.17982   0.56907   0.97558   1.3987   1.8367   2.4271
 1
 1   1   144
 11.66
 12.6885   0.276
 20   20   15
 0.02   0.5   1   5   10   15   50
 0.03
 0.5  -0.5   600   30
 1 0.8237 0.6696 0.5361 0.4216
 25.377   1
 0   1   0   300   0   0   1
**Panel 1 (300 elements)
 0   0   0   0
-12.563   12.813  -2.094   15.722   3.518   50.884
 0   0   31   11   0
 0   0.1   0.2   0.3   0.4   0.5
 0.6   0.7   0.8   0.9   1
 0   0.0333   0.0666   0.0999   0.1332   0.1665
 0.1998   0.2331   0.2664   0.2997   0.333   0.3663
 0.3996   0.4329   0.4662   0.4995   0.5328   0.5661
 0.5994   0.6327   0.666   0.6993   0.7326   0.7659
 0.7992   0.8325   0.8658   0.8991   0.9324   0.9657
 1
 1   0   0   0   0   0
 1   300   0
F  300   0
 3   0   1   1
**LINE1
 7  -6.939   0   2.133   50.884
 7.92   13.04   17.96   22.88   27.8   32.7   39.15
**LINE2
 7  -0.987   0   8.133   50.884
 7.92   13.04   17.96   22.88   27.8   32.7   39.15
**LINE3
 7   8.65   0   12.477   50.884
 7.92   13.04   17.96   22.88   27.8   32.7   39.15
 0
```

```
 1
Flutter analysis of JS1 sailplane: Tailplane
Multi panel with  155  elements
No control surfaces
P-K flutter type
 1  vibration modes: Symm
mach=1.2xVd
-1   1   1   6   5   0   0   0   0   0
 1   0   1   0   0   1   0   0   1   0
 1   0   0   1   0   0   0   0   0   0
 0   0   0   0   0   0   1
 15
-0.5108  -1.9871  -4.6329  -7.0711  -10.211  -0.55551  -2.0829
-4.7289  -7.2045  -10.333  -0.55731  -2.1176  -4.7887  -7.3263
-10.459
 1
 1   1   144
 19.213
 8.2075   0.276
 20   20   15
 0.02   0.5   1   5   10   15   50
 0.03
 0.5  -0.5   600   30
 1   0.8237   0.6696   0.5361   0.4216
 16.415   1
 1   5   0   155   0   0   1
**Panel 1 (40 elements)
 0   0   0   0
-8.187   8.229  -6.974   7.345   2.737   24.194
 0   0   9   6   0
 0   0.2   0.4   0.6   0.8   1
 0   0.125   0.25   0.375   0.5   0.625
 0.75   0.875   1
**Panel 2 (40 elements)
 0   0   0   0
-6.974   7.345  -4.906   6.603   24.194   41.871
 0   0   9   6   0
 0   0.2   0.4   0.6   0.8   1
 0   0.125   0.25   0.375   0.5   0.625
 0.75   0.875   1
**Panel 3 (30 elements)
 0   0   0   0
-4.906   6.603  -1.549   6.047   41.871   55.118
 0   0   7   6   0
 0   0.2   0.4   0.6   0.8   1
 0   0.16667   0.33334   0.50001   0.66668   0.83335
 1
**Panel 4 (15 elements)
 0   0   0   0
-1.549   6.047   0.976   5.779   55.118   58.866
 0   0   4   6   0
 0   0.2   0.4   0.6   0.8   1
 0   0.3333   0.6666   1
**Panel 5 (30 elements)
 0   0   0   0
 0.976   5.779   4.787   5.574   58.866   60.74
 0   0   7   6   0
 0   0.2   0.4   0.6   0.8   1
 0   0.16667   0.33334   0.50001   0.66668   0.83335
 1
 1   0   0   0   0   0
 1   155   0
F  155   0
 3   0   1   1
**LINE1
 5  -4.495   0  -1.549   58.866
 10.24   19.99   31.26   40.1   49.82
**LINE2
 5   0.691   0   0.772   58.866
 10.24   19.99   31.26   40.1   49.82
**LINE3
 5   4.442   0   3.852   58.866
 10.24   19.99   31.26   40.1   49.82
 0
```

A3: Flutter diagrams

Configuration	Components				Total Weight
1	Fuselage	Wings	-	-	400
2	Fuselage	Wings	Engine	-	500
3	Fuselage	Wings	Engine	Water (92kg)	600
4	Fuselage	Wings	-	Water (200kg)	600

Configuration 2: Symmetrical Modes

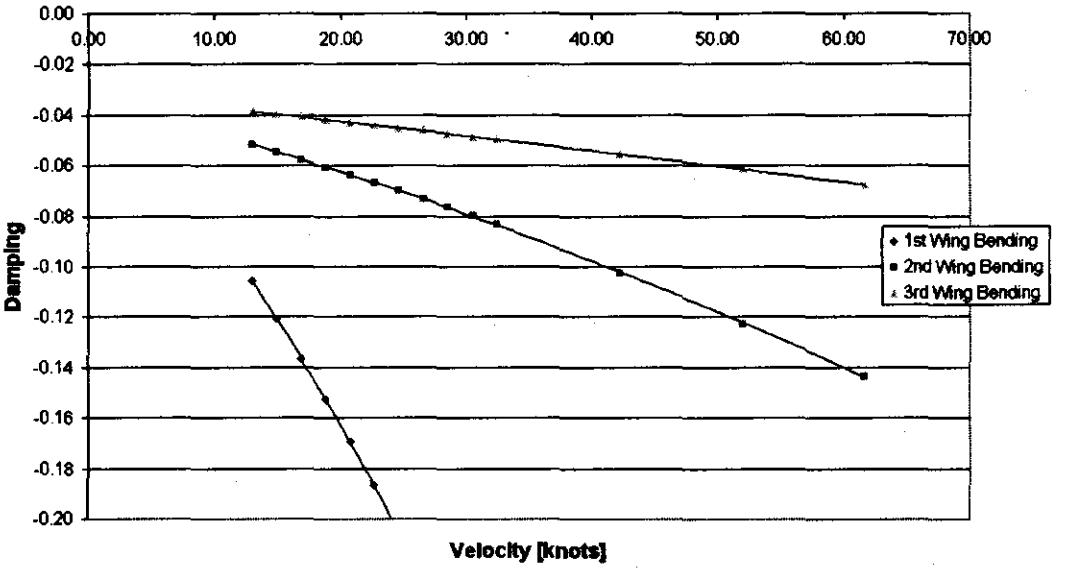

Configuration 2: Symmetrical modes

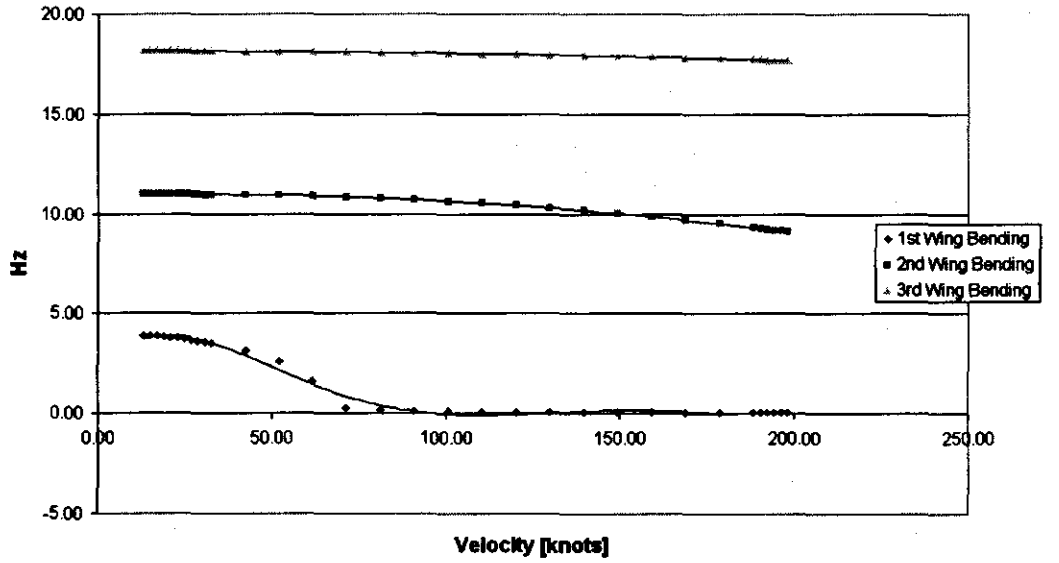

Configuration 2: Asymmetrical Modes

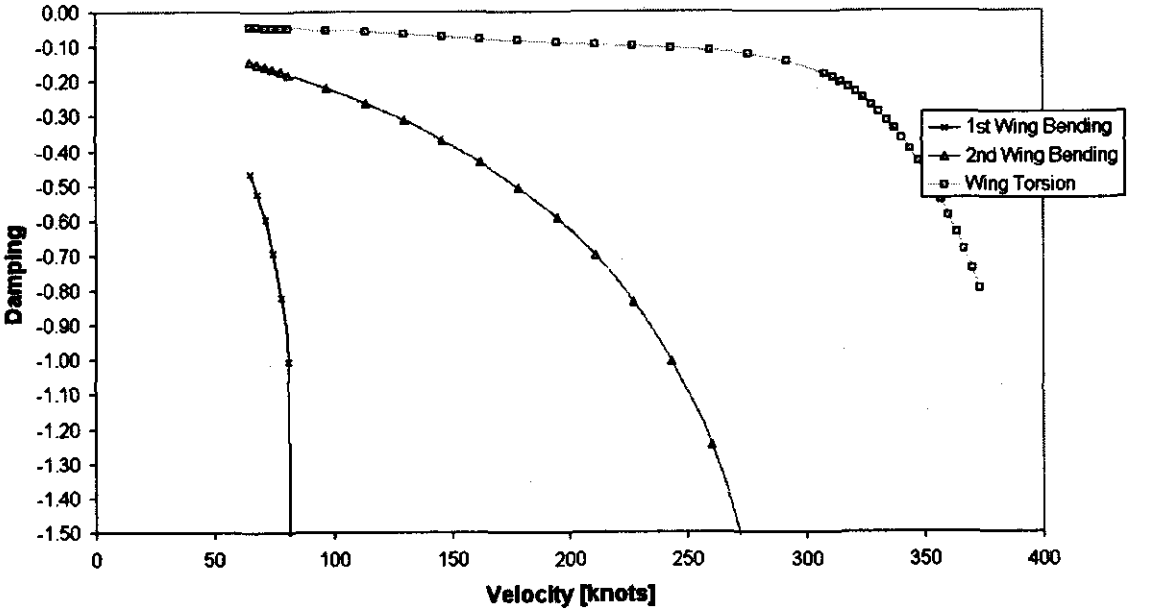

Configuration 2: Asymmetrical Modes

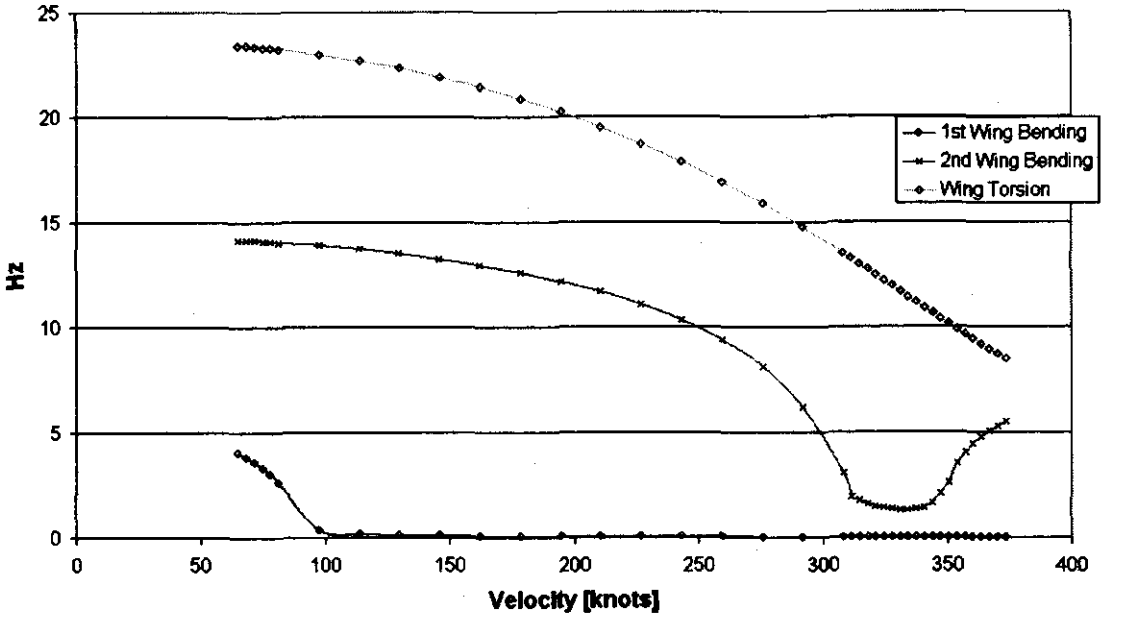

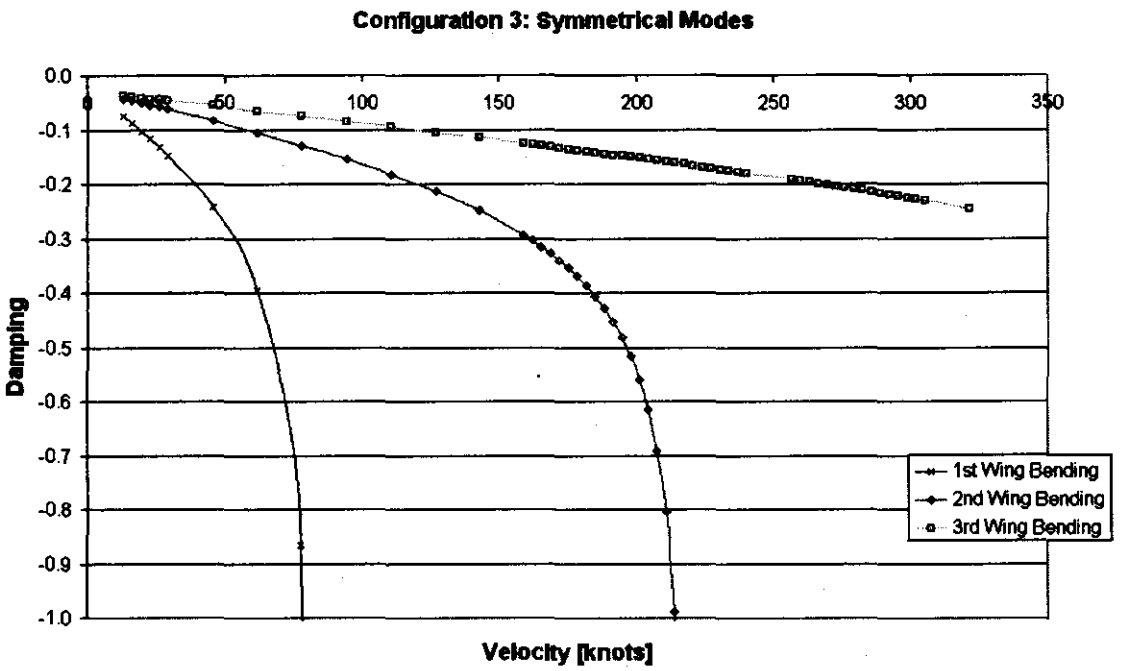
Configuration 3: Symmetrical Modes
0.0
-0.1
-0.2
-0.3
-0.4
-0.5
-0.6
-0.7
-0.8
-0.9
-1.0
Damping
0
50
100
150
200
250
300
350
Velocity [knots]
1st Wing Bending
2nd Wing Bending
3rd Wing Bending

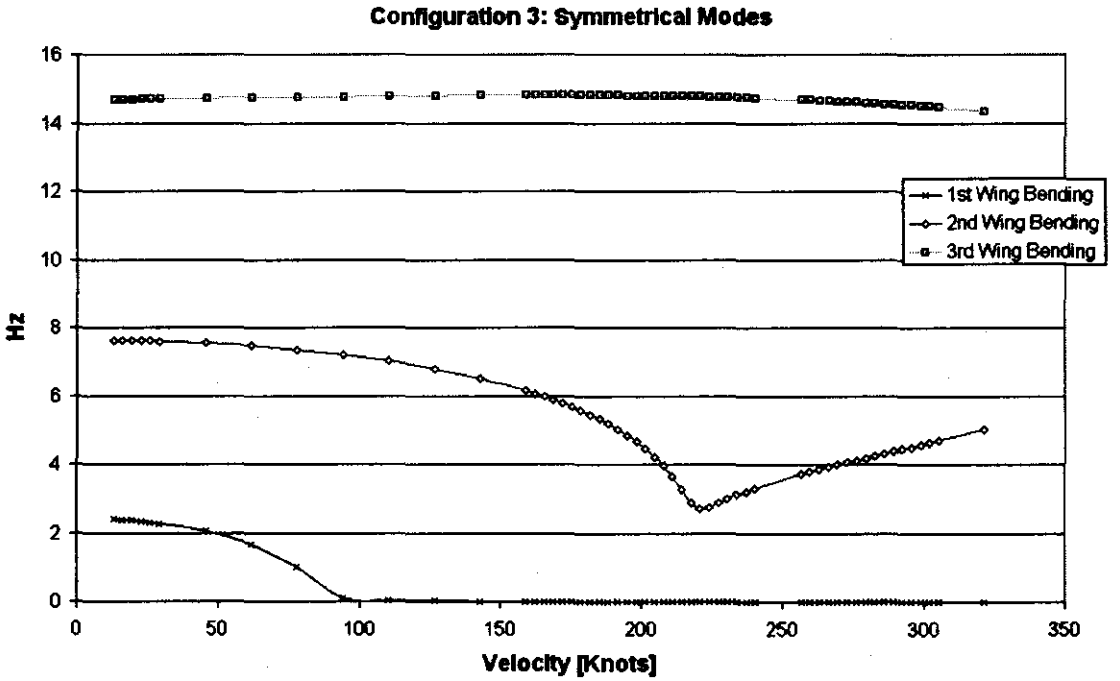
Configuration 3: Symmetrical Modes
16
14
12
10
8
6
4
2
0
Hz
0
50
100
150
200
250
300
350
Velocity [Knots]
1st Wing Bending
2nd Wing Bending
3rd Wing Bending

Config 3: Asymmetrical Modes

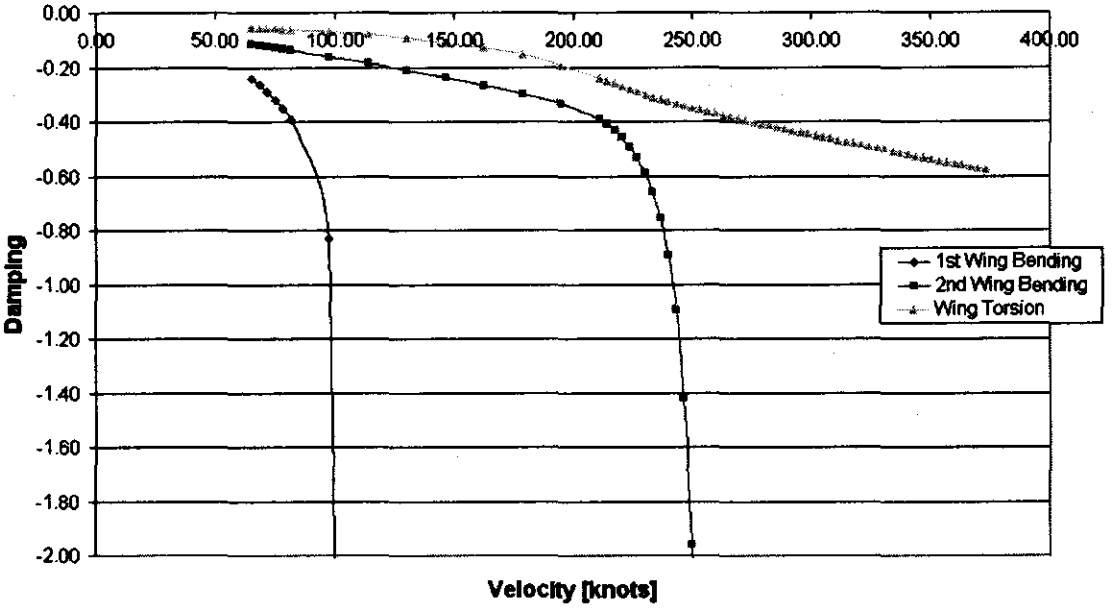

Configuration 3: Asymmetrical Modes

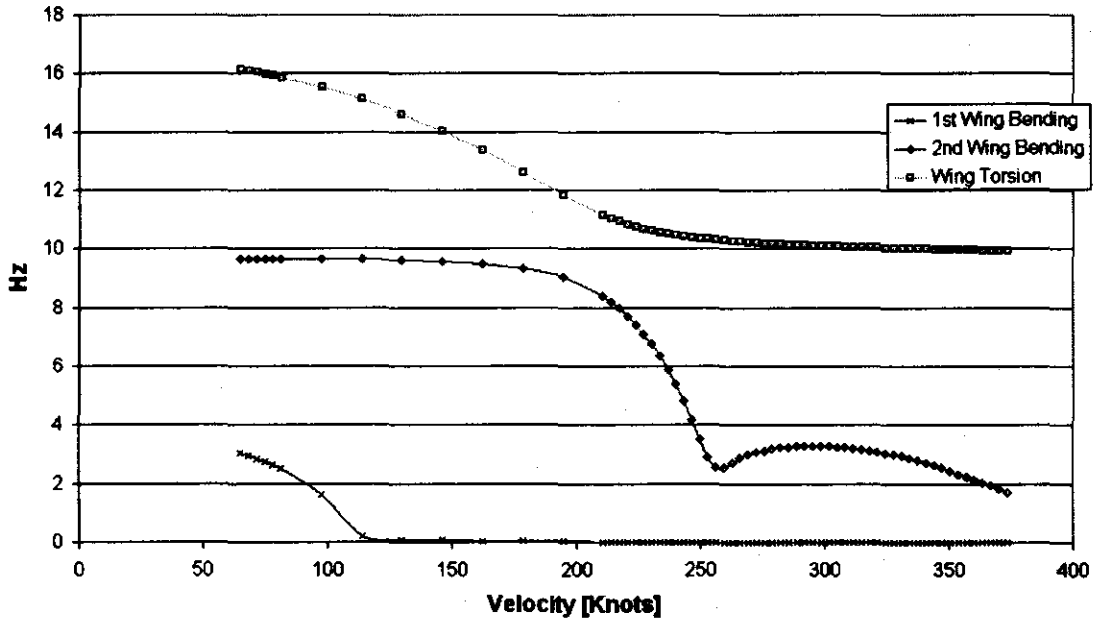

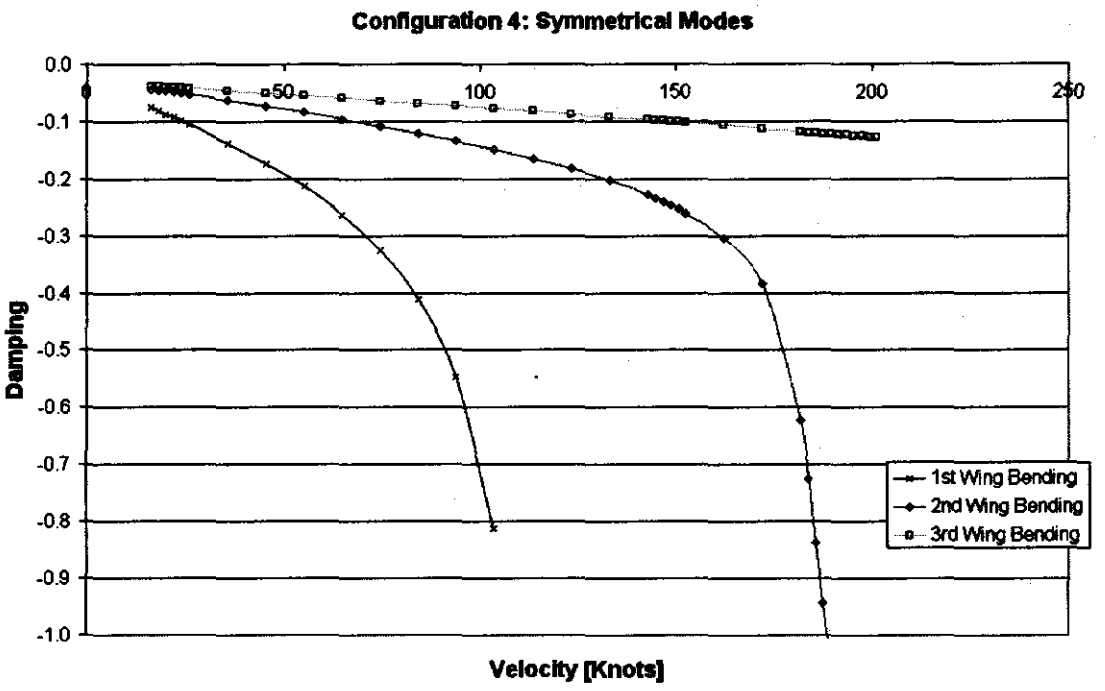
Configuration 4: Symmetrical Modes
0.0
-0.1
-0.2
-0.3
-0.4
-0.5
-0.6
-0.7
-0.8
-0.9
-1.0
Damping
0
50
100
150
200
250
Velocity [Knots]
1st Wing Bending
2nd Wing Bending
3rd Wing Bending

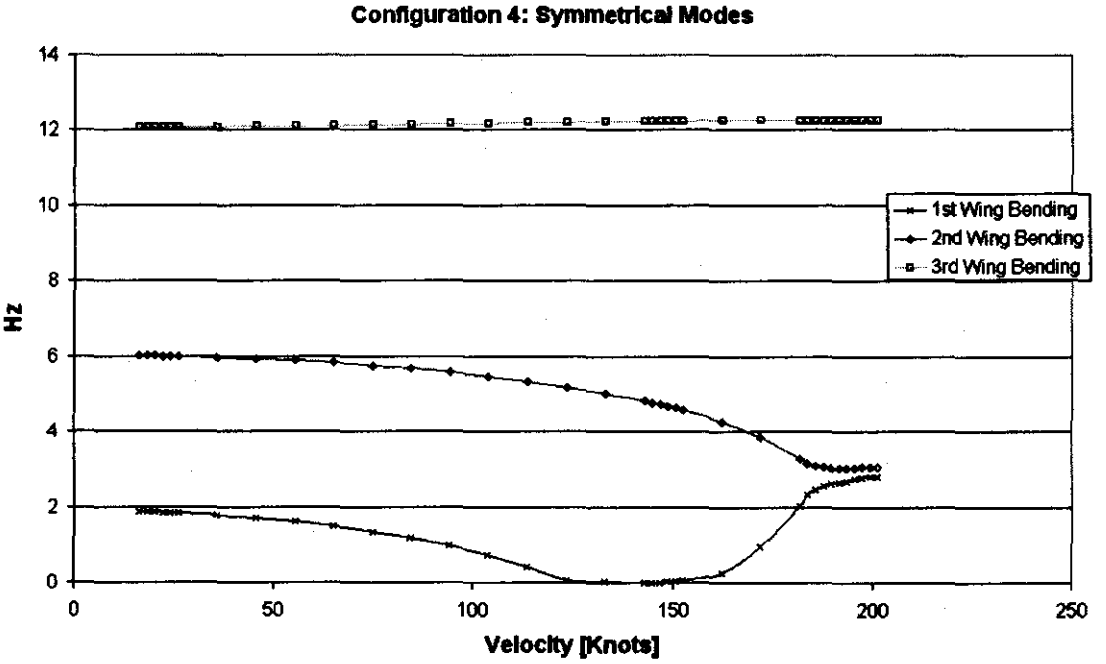
Configuration 4: Symmetrical Modes
14
12
10
8
6
4
2
0
Hz
0
50
100
150
200
250
Velocity [Knots]
1st Wing Bending
2nd Wing Bending
3rd Wing Bending

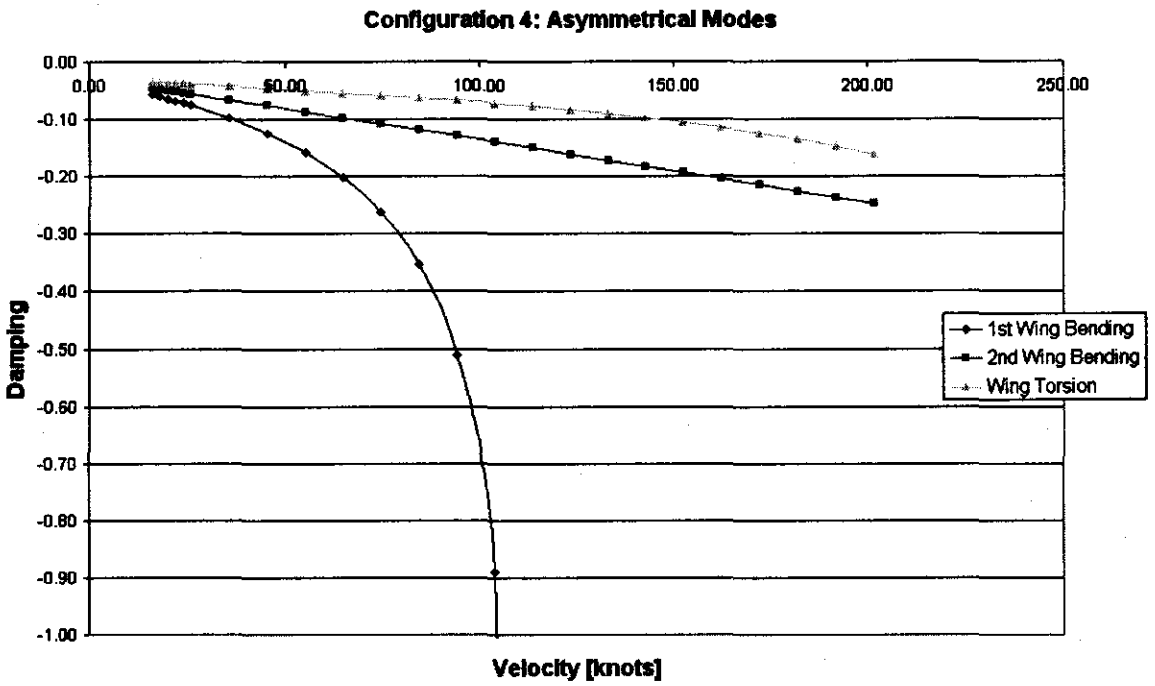
Configuration 4: Asymmetrical Modes
0.00
-0.10
-0.20
-0.30
-0.40
-0.50
-0.60
-0.70
-0.80
-0.90
-1.00
Damping
0.00
50.00
100.00
150.00
200.00
250.00
Velocity [knots]
1st Wing Bending
2nd Wing Bending
Wing Torsion

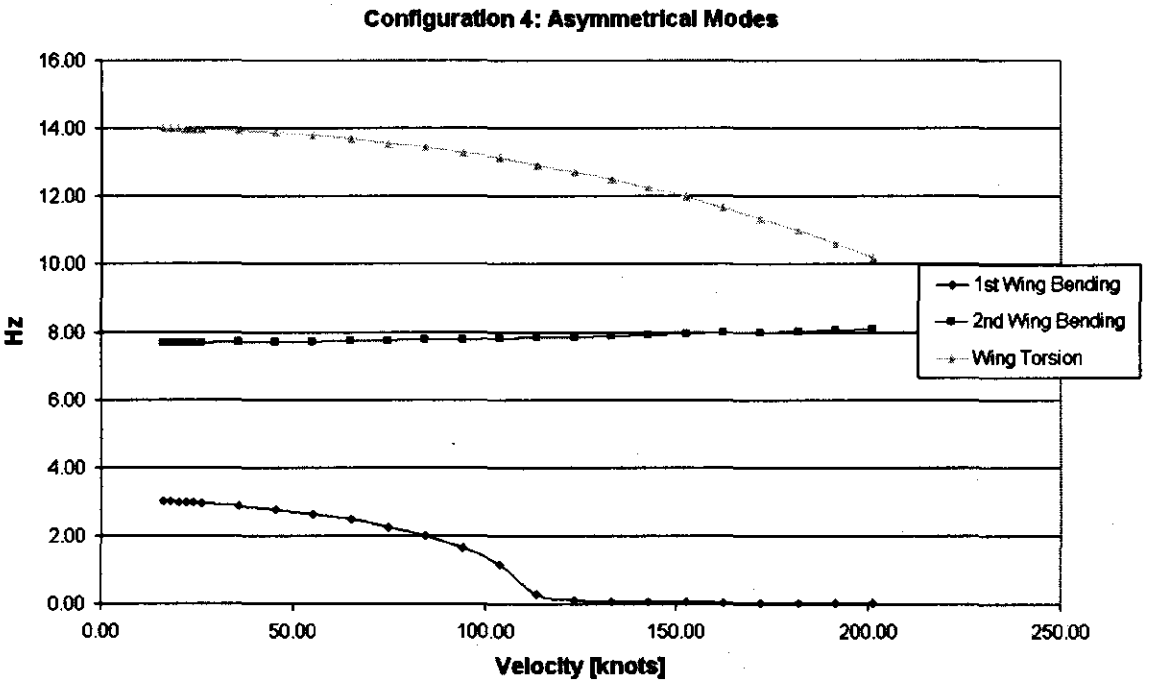
Configuration 4: Asymmetrical Modes
16.00
14.00
12.00
10.00
8.00
6.00
4.00
2.00
0.00
Hz
0.00
50.00
100.00
150.00
200.00
250.00
Velocity [knots]
1st Wing Bending
2nd Wing Bending
Wing Torsion

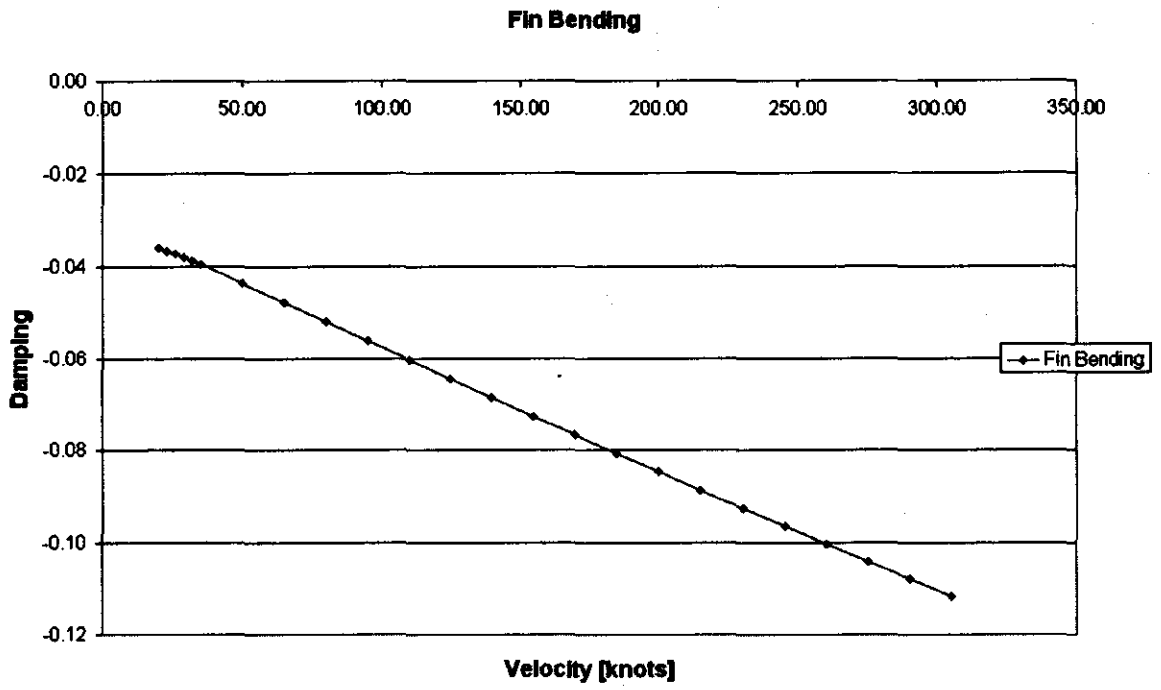
Fin Bending
0.00
-0.02
-0.04
-0.06
-0.08
-0.10
-0.12
Damping
0.00
50.00
100.00
150.00
200.00
250.00
300.00
350.00
Velocity [knots]
Fin Bending

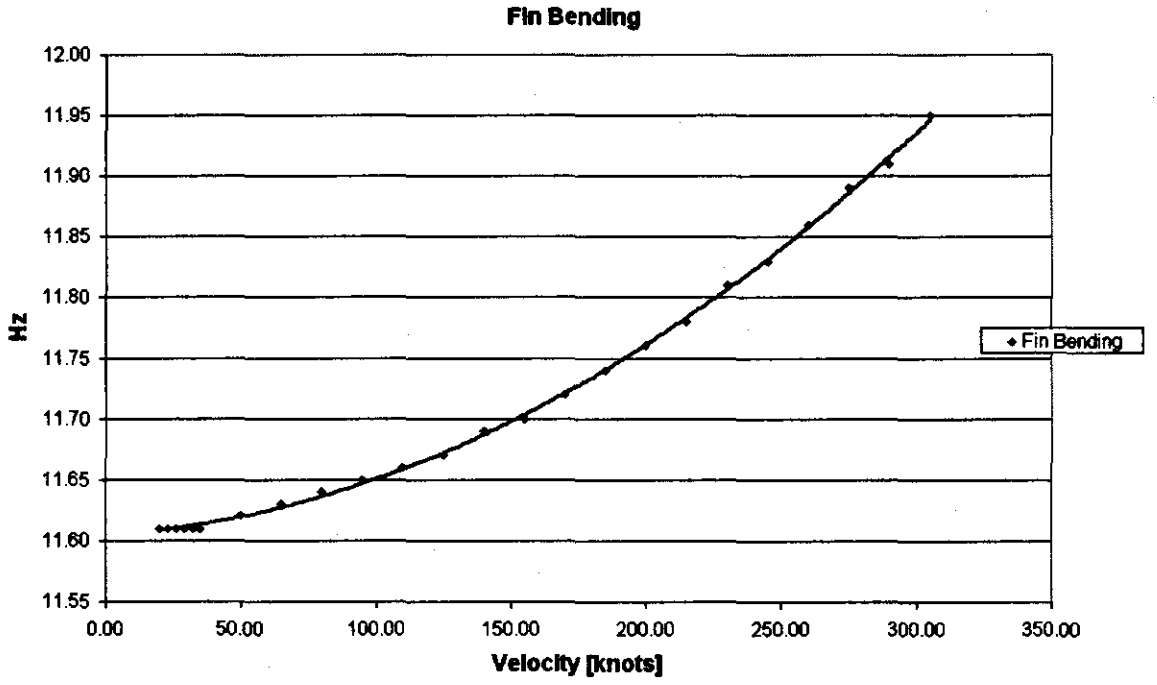
Fin Bending
12.00
11.95
11.90
11.85
11.80
11.75
11.70
11.65
11.60
11.55
Hz
0.00
50.00
100.00
150.00
200.00
250.00
300.00
350.00
Velocity [knots]
Fin Bending

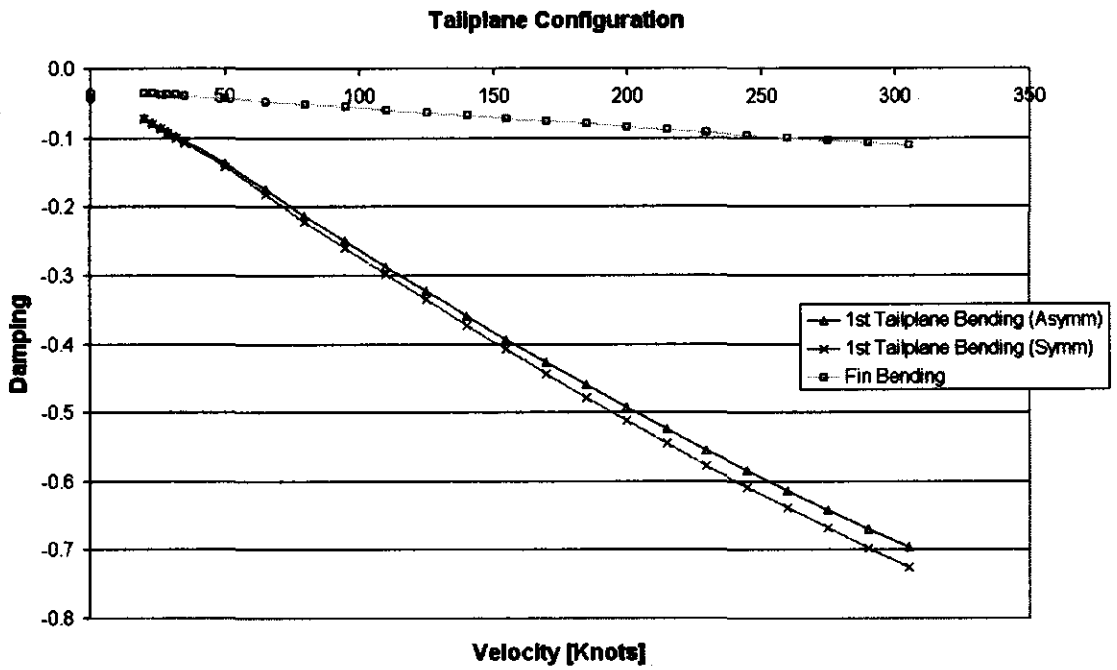
Tailplane Configuration
0.0
-0.1
-0.2
-0.3
-0.4
-0.5
-0.6
-0.7
-0.8
Damping
0
50
100
150
200
250
300
350
Velocity [Knots]
1st Tailplane Bending (Asymm)
1st Tailplane Bending (Symm)
Fin Bending

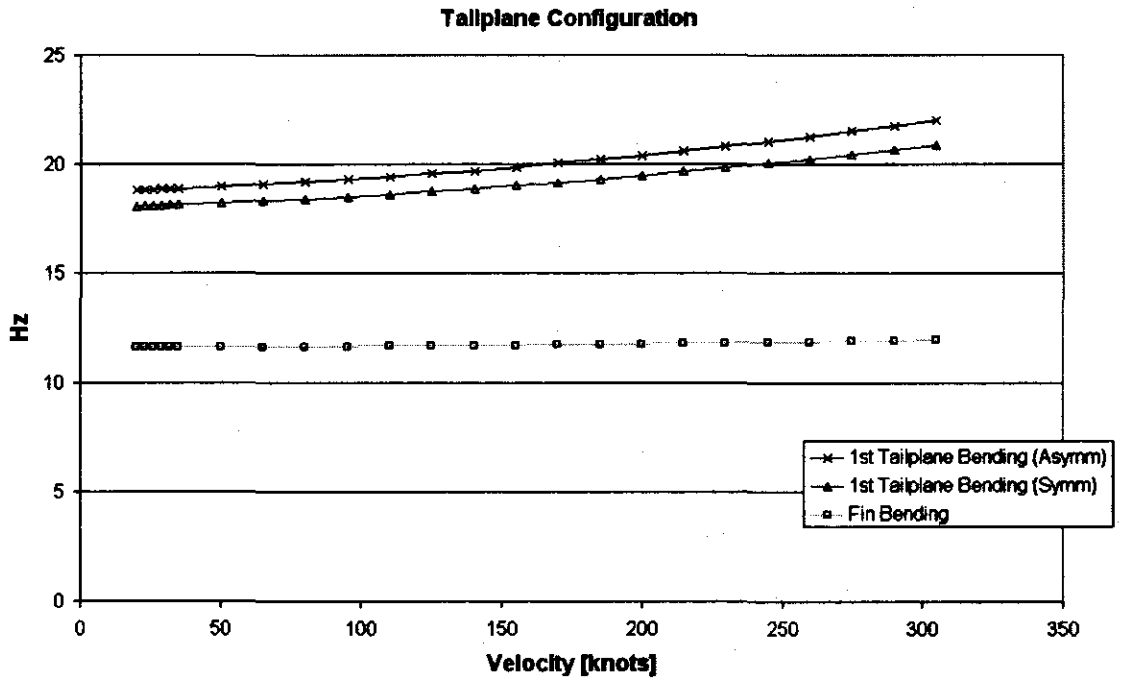
Tailplane Configuration
25
20
15
10
5
0
Hz
0
50
100
150
200
250
300
350
Velocity [knots]
1st Tailplane Bending (Asymm)
1st Tailplane Bending (Symm)
Fin Bending

A4: JS1 18m-Sailplane

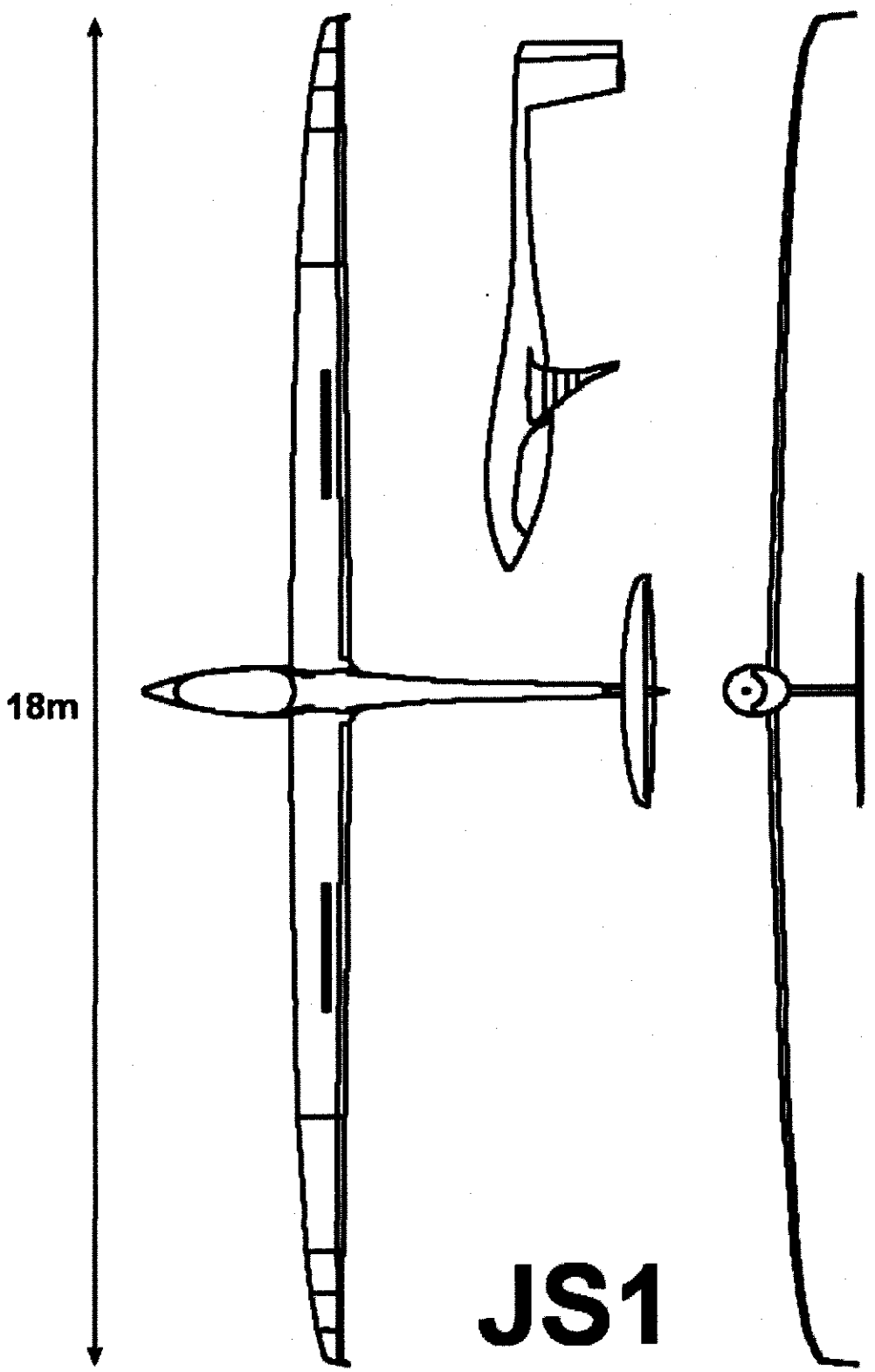

Bibliography

ANSYS Inc. 2000. **Element Library.** ANSYS Inc. USA.

Bosman, J.J. 2001. **The design and optimization of an 18m class glider wing with the use of numerical methods.** Potchefstroom, South Africa.

Collar, A.R. 1978. **The first fifty years of aeroelasticity.** Aerospace, 5(2): p.12-20, Feb.

Dowell, E.H., Crawley, E.F. & Curtiss, H.C. 1995. **A modern course in aeroelasticity.** Netherlands: Kluwer Academic Publishers. 699p.

Garrick, I.E. & Reed, W.H. 1981. **Historical development of aircraft flutter.** *AIAA,* 18(11): p. 897-912, Nov.

Hassig, H.J. 1971. **An approximate true damping solution of the flutter equation by determinant iteration.** *Journal of Aircraft*, 8(11)

Hodges, D.H. & Pierce, G.A. 2002. **Introduction to structural dynamics and aeroelasticity.** New York: Cambridge University Press. 109p.

Hollmann, M. 1997. **Modern aerodynamic flutter analysis.** Aircraft Design Inc.: Monterey, California. 168p.

Joint Aviation Authorities. 2003. **JAR-22 Sailplanes and Powered Sailplanes.** Joint Aviation Authorities. Netherlands.

Kehoe, M.W. 1995. **A historical overview of flight flutter testing.** *NASA Technical Memorandum 4720:* p1-17, Oct.

Kimberlin, R.D. 2003. **Flight testing of fixed-wing aircraft.** Reston: American Institute of Aeronautics and Astronautics. 439p.

Kühn, G.C. 2003. **The Structural design of the tailplane of the JS1 glider.** Potchefstroom. South Africa

Laure, P. & Millet, M. 1974. **Pyrotechnic bonkers for structural tests in flight.** *ONERA*, 1389.

Lind, R. 2001. **Flight test evaluation of flutter prediction methods.** *Journal of aircraft*: Jun.

Lind, R. & Brenner, M. 1999. **Robust aeroservolastic stability analysis.** Springer-Verlag, London: April

Lind, R. & Brenner, M. 2000. **Flutterometer: an online tool to predict robust flutter margins.** *Journal of aircraft*, 37(6): p.1105-1112, Nov.

Maurice, P. 1998. **Introduction to finite element vibration analysis.** United Kingdom: Cambridge University Press.

Meirovitch, L. 1970. **Methods of analytical dynamics.** New York: McGraw-Hill.

Nordwall, B.D. 1993. **Mobile Communication to capture consumer market.** *Aviation Week & Space Technology.* p. 41-42, May.

Petyt, M. 1990. **Introduction to Finite Element vibration analysis.** Australia: Cambridge University Press. 553p.

Philbrick, J. 1958. **Experience in flight flutter testing.** *Proceedings of 1958 flight flutter testing symposium:* p.127-132.

Robinson, J. 1985. **Basic and shape sensitivity tests for membrane and plate bending finite elements.** *NAFEMS C2:* National Engineering Laboratory Report.

Shokrieh, M.M. & Behrooz, F.T. 2001. **Wing instability of a full composite aircraft.** *Composite Structures*, 54: p.335-340.

Stringham, R.H. & Lenk, E.J. 1958. Flight **flutter testing using pulse techniques.** *Proceedings of the 1958 Flight Flutter Testing Symposium.* p. 69-72.

Theodorsen, T. 1935. **General Theory of aerodynamic instability and the mechanism of flutter.** *NACA Report*, 496.

Tolve, L.A. 1958. **Historical development of aircraft flutter.** *Technical proceedings of the 1958 flight flutter testing symposium*: p.159-166.

Van Zyl, L.H. (LvZyl@csir.co.za) 2003. **Flutter Information**: [E-mail to:] De Bruyn, J.A. (mgijadb@puk.ac.za)

Von Schlippe, B. 1936. **The question of spontaneous wing oscillations.** *NACA:* Oct.

Wilkinson, K. et al. 1975. **An automated procedure for flutter and strength analysis and optimization of aerospace vehicles.** *AFFDL-TR-75-137*, 1&2: Dec.